A review on shape memory metallic alloys and their critical stress for twinning

P. Nnamchi, A. Younes, S. González

Faculty of Engineering and Environment, Northumbria University, Newcastle upon Tyne NE1 8ST, United Kingdom

Abstract

Shape Memory Alloys (SMAs) is a class of smart materials with the ability to remember the original shape. SMAs exhibit stress-induced martensitic transformation through twinning which is an important deformation mechanism that renders strength and ductility. Tailoring the capability of alloys for deformation twinning enables to optimize their mechanical performance. This paper presents a comprehensive review on the effect of internal and external parameters on the twinning propensity. Among these parameters, the effect of the composition, grain size, temperature and strain rate will be explored. In addition the use of shape memory phase as a strategy to improve the ductility of metallic use memory behaviour is of great importance to develop SMAs for multiple applications including mechanical, automotive, aerospace, civil and biomedical industries. A tentative outlook about the challenges and proposed solutions will be also discussed.

1. Introduction

Shape Memory Alloys (SMAs) are special materials with great potential in various engineering applications since they possess a number of unique characteristics, including superior energy dissipation capacity compared to normal metallic materials.

The first SMAs were discovered in gold-cadmium (Au–Cd) alloys in 1932 by a Swedish physicist named Arne Ölander [1] and subsequently, in 1938, Greninger and Mooradian [2] observed similar property in copper-zinc (Cu–Zn) and copper-tin (Cu–Sn) alloys. Nonetheless, the term ‘‘shape-memory’’ was not coined until 1941 when Vernon used this name to his polymeric dental material [3]. The importance and the demand of SMAs for most engineering and technical applications was not positively realised, until the discovery of the shape memory effect (SME) in a nickel-titanium (NiTi) alloy by William Buehler and Frederick Wang in 1962 [4]. This equiatomic alloy is also known as nitinol (derived from the material composition and the place of discovery, i.e. a combination of NiTi and Naval Ordnance Laboratory, part of the US Department of Defence). Thereafter,

the use of SMAs, has expanded and the research interests and patents have become quite large. Examples of the possible beneficiaries of these materials abound in a variety of fields, such as automobile and mechanical engineering applications, [5, 6], automotive [5], aerospace [7], mini actuators and micro-electromechanical systems (MEMS) [8], robotics [9], biomedical [10] and even in clothing / fashion industries [11]. Albeit Shape Memory metals were initially developed by NASA for the space industry, it has been used for increasing applications down on earth.

The interest in using shape memory alloys (SMAs) stems from the fact that they can "remember" their original shape. When subjected to an external force above a threshold, they exhibit stress-induced martensitic transformation from austenite into martensite through twinning, and can recover the apparent permanent strains, returning to the original form. Twinning can be defined as the coordinated motion of planes of atoms parallel to the twinning plane so that the lattice is divided into two symmetrical domains with the same crystalline structure (see schematic in Fig.1) but these domains are mirror image of each other [12, 13]. The boundaries (i.e., twinning plane) represent a particularly symmetric kind of grain boundary but with much lower level of interfacial energy than that of general grain boundaries. Twinning is commonly observed during solidification, deformation, solid-state phase transformation and recrystallization in a variety of crystalline solids with low crystal symmetry such as body centered cubic (bcc), hexagonal close packed (hcp), lower symmetry metals and alloys [14] and some nanoscale metals [15, 16]. Twinning has also been detected in face centred cubic (fcc) metals and alloys when the Stacking Fault Energy (SFE) is low, such as in Cu (70-78 J/m^2) or even in high SFE elements such as Al (160- 200J/m^2) although only when subjected to very high rates of loading such as in case of explosions. Twinning, as deformation dislocation slip, is a fundamental plastic deformation mode in crystalline solids [14] that enables a solid to change shape under stress. Twinning takes place when there is a lack of easily activated independent slip systems and therefore when, for the applied stress, it is easier to nucleate and propagate twins rather than dislocations. Twinning can be promoted by decreasing the SFE since when the SFE is low the mobility of dislocations in a material decreases. This is useful to promote deformation twinning since it can provide a substantial work hardening and a twinning-induced plasticity (TWIP) effect. Thus, the introduction of deformation twinning by tailoring the stacking fault energy is an important mode of plastic deformation in fcc TWIP steels [17] and it has become an important approach for enhancing both strength and ductility.

Martensite twinning and subsequent recovery upon heating is called “shape memory effect” [18]. This effect has the curious property of returning the material to its original shape by heating it up after having been permanently deformed at room temperature. However, for this process to take place, the crystal structures should possess very little slip possibilities since the slip process is irreversible (i.e., it is not possible to return a crystal structure into its exact original configuration). The present interest in the phenomenon of twinning arose from its importance to simultaneously improve the strength and ductility of traditional materials. This idea has been recently applied as a strategy to improve the ductility of more new materials such as bulk metallic glasses (BMGs), particularly (CuZr)- and Ni-Ti-based BMGs by developing composites [19]. These composites combine the ductility, fracture toughness and plasticity of shape memory crystalline phase with the high strength of monolithic BMGs because the dispersed particles of austenitic phase undergo stress-induced martensitic transformation thus resulting in work-hardening and therefore can prevent catastrophic failure caused by strain softening of the amorphous matrix. Martensitic transformation takes place in a diffusionless manner caused by a shear force of specific magnitude. This results in the movement of some atoms in part of the parent over a small distance relative to its neighbours so that the atoms reorient into a mirror orientation. Subsequent deformation creates new twins while the plains of existing twins propagate normal to themselves so as to be compatible with the gross change of shape. Upon heating, the twinning plain moves back to their original position causing a return to the original shape. A detailed explanation of the process for the crystal lattice of nitinol, i.e., NiTi shape memory alloy, was reported by Wang [20] who suggested that the formation of all twins involve co-operative shear where all the atoms move in the same direction parallel to the plane of twin boundries. Despite the interest of shape memory materials in multiple engineering applications, the number of manuscripts dealing on how to tune their performance is scarce and fragmented. For this reason this manuscript aims to provide a comprehensive updated review on twinning and a systematic analysis about the different parameters to tune the twinning propensity so that it can be used as a guideline. Due to the importance of parameters such as temperature, grain size, texture, composition (i.e., alloying and microalloying) and strain rate on the twinning and martensitic behaviour of shape memory materials their, effect will be discussed. Finally, the importance of twinning as a strategy to improve the performance of engineering materials and metallic glasses will be explored.

1.1. Brief description of twinning and detwinning process in Shape Memory Alloys

Over the past few decades, several key works have explored the microstructural mechanisms, engineering effects and applications of shape memory alloys [21], including the comprehensive summary of Otsuka et al. [22]. The shape memory effect and superelasticity (or pseudo elasticity) are the most frequently used phenomena. Both behaviours are a consequence of the reversible nature of the martensitic transformation achieved through the motion of twin boundaries, i.e., reorientation of martensite variants. Twinning and detwinning are important microstructural processes partially responsible for shape memory effect and superelasticity in shape memory alloys [23].

One may ask, why do some materials exhibit shape memory effect while others do not? One major distinction between these two types of materials is the deformation mechanism. When the latter is stressed beyond its yield limit in martensite, dislocations are generated and are responsible for the observed plastic deformation. However, in the former, the dislocations generated are insignificant because the critical stress for activating the detwinning process is lower than that for dislocation generation and, owing to an insignificant dislocation process, the associated shape change can be partially or even fully restored through a reverse phase transformation [24]. The observed inelastic deformations when martensitic SMA is stressed beyond its yield limit is due to this "detwinning" process. This inelastic deformation can reach about 6 % strain without a significant increase in dislocation density [25].

SMAs have two phases within the typical operating temperature range, each with a different crystal structure and therefore different properties. The high temperature phase known as the austenite phase (A) (i.e., the parent or memory phase) with long-range order and the other is the low temperature phase called martensite (M). Austenite is generally cubic and has a different crystal structure from martensite (tetragonal, orthorhombic or monoclinic). This crystallographic reversible phase transformation from austenite into martensite and vice versa forms the basis for the unique behaviour of SMAs [4]. Shape Memory Alloys (SMAs) are a unique class of materials because of their ability to recover their shape when the temperature is increased. Upon cooling below the transformation temperature, the austenite transforms into a thermoelastic martensite whose structure has many variants, typically sheared platelets. SMAs can recover also large amounts of stress induced inelastic deformation immediately upon unloading. However, if the material is tested just above its transformation temperature to austenite (A_f), the applied stress transforms the austenite to martensite and the material exhibits increasing strain at

constant applied stress therefore resulting in high actuation energy densities, i.e. considerable deformation occurs for a relatively small-applied stress. When the stress is removed, the martensite reverts to austenite and the material recovers its original shape. This effect is known as superelasticity or pseudoelasticity and makes the alloy appear extremely elastic, [26]. Each martensitic crystal formed can have different orientation direction called variant. The assembly of martensitic variants can exist in two forms: twinned martensite (M_t), which is formed by a combination of "self-accommodated" martensitic variants and detwinned or reoriented martensite, in which a specific variant is dominant (M_d). The martensite deforms through a twinning mechanism that transforms the different variants to the variant that can accommodate the maximum elongation in the direction of the applied force [27]. The interfaces between platelets in the martensite phase glide very readily and the material is deformed at low applied stresses. The austenite phase has only one possible orientation, for this reason, when heated up, all the possible deformed structures of the martensite phase must revert to this one orientation of the austenite memory phase and the material recovers its original shape. The maximum shape recovery strain is intrinsically related to the lattice geometry and twinning mode, while the magnitude of shape recovery is related to a competition between detwinning and dislocation generation responsible for the macroscopically observed deformation [28]. Altogether, it can be asserted that shape memory effect and superelastic property are direct effect of detwinning and coalescence of twinning process.

1.2. Twinning nucleation mechanisms

The initial explanation of twinning nucleation mechanisms was centred on classical nucleation, since its first discovery coincided with the development of the classical nucleation theory. It is generally regarded that twinning occurs through a process of nucleation and growth and therefore separate attention should be given to each of them. Orowan et al. [29] first proposed a model for homogeneous nucleation of a twin and it was used to explain the experimental results observed in nearly perfect crystals. In this model the free-energy barrier for twin nucleation is overcomed by thermal fluctuation. However, experimental evidence to support such claim of thermally activated mechanism does not exist and it is contradictory to observations of increased twinning during deformation at very low temperatures. In addition, other theoretical arguments in support of homogeneous nucleation remain quite unclear and they hardly explain how twins can nucleate by homogeneous nucleation mechanism [30], for this reason only a few authors have studied

this process. For example, the possibility of homogeneous nucleation of twins in near perfect hcp crystals was reported by Bell and Cahn [31] and also by Price [32]. Their results, however, can also be attributed to the initiation of twinning due to the presence of some defect configuration, because much higher stress would be required to achieve homogeneous nucleation. This means that for homogeneous nucleation twinning to take place, the applied shear stress has to be high enough to reach a critical value, the so-called theoretical strength of a material (i.e., maximum possible stress a perfect solid can withstand). Therefore, it can be concluded that spontaneous homogeneous nucleation of twins in defect-free regions under the influence of applied stress is very improbable, unless there is a combination of very high stress and very low surface and strain energies [33].
Several twinning mechanisms have been proposed and observed in metals and alloys over the years [14] to interpret the mechanisms of twinning nucleation specific to a lattice structure, including the pole mechanism [34], prismatic glide mechanism [35], faulted dipole mechanism [36] and other multiple mechanisms [37].

1.3. Homogeneous and heterogeneous nucleation mechanisms

This mechanism assumes homogenous nucleation in the vicinity of stress concentrators but pontaneous formation of a large twin volume is energetically unlikely. In line with typical engineering alloys, heterogeneous nucleation (defect assisted) of twins at grain boundaries or dislocations is more likely [14] than homogeneous nucleation, where a combination of very high stresses and low surface and strain energies [38] are required.

Previously, the potential influence of defects on twin nucleation has been studied from classical experiments [32, 39] and from theoretical calculations [40]. These heterogeneous nucleation studies suggest that twins may form only when at least a single or suitable defect configuration is present. Initially, pre-existing dislocation configurations split up into separate or multi-layered stacking fault structures which serve as twin nucleus. Subsequent growth could happen by random accumulation of independently collected stacking faults over time. Thus, a widespread twin growth must involve repeated split ups of multi-layered stacking fault defect structures into favourable twins [41]. For example, Price [42] analysed single hcp zinc crystals (without the defects associated to grain boundaries of polycrystalline materials) stressed to a much higher levels than those at which twins normally form in less perfect crystals to demonstrate that twins can be induced in a highly stressed crystal. This relates to the size of the specimen tested since the larger it is, the higher the probability to contain defects and therefore to exhibit heterogeneous

twin nucleation. The result indicates that twin nucleation occurs in a region where the applied stress is concentrated, such as specimen grips, at a corrosion pit or at a growth step. The author found that the stresses required to induce twinning were an order of magnitude higher than those usually measured in other macroscopic specimens [32]. However, the critical resolved shear stress for twinning (i.e., ~ 50 Kg/mm^2) was comparable to the value of the theoretical twinning stress. Similarly, it was observed that platelets of cadmium deformed in tension parallel to the basal plane, inside an electron microscope, in the temperature range from 25° to -150°C twinned at high stresses [41].

The number of slip systems in a crystal structure also determines whether dislocation slip or twinning are more likely to occur. For hcp crystal structure it depends on the axial c/a ratio, where a is the lateral and c the base parameter, respectively. For example, Cadmium and Zinc in their pure metal form, have a ratio of c/a >1.63 where the 6 nearest neighbours in the basal plane and 3 nearest neighbours above, and below the basal plane at slightly greater distances. For other hcp metals where c/a <1.633 have 3 atoms above and below at slightly closer distances than those in the basal plane. The intrinsic Peierls-Nabarro stress required for slip or twinning is expected to be smaller for planes having the largest interplanar spacing, as in the case of Cd and Zn (i.e. low index planes containing the greatest density of atoms) and containing the shortest lattice translation vectors, which may explain the reason for the lower stress required to induce twinning.

1.4. Pole (Single dislocation) mechanism

Pole mechanism assumes that heterogeneous nucleation of twins occur due to splitting of a dislocation in the twinning plane, where the leading partial twinning dislocation is glissile. Subsequently a twin can then grow from the nucleus by a pole mechanism (i.e. by the rotation of the twinning dislocation round a node). However, this is only feasible if the dislocation configuration at the node is able to give a suitable screw component of the burger vector that will enable the twinning plane change into a helical surface. This mechanism was proposed by Cottrell and Bilby in 1951 [43] to account for twinning the creation of combined nucleation and growth mechanism in bcc and extended by Venables in 1961 [35] for fcc crystals. The author proposed that twins nucleate from a single stacking fault. However, Sleeswyk pointed out that a perfect pole twin can be obtained in fcc crystals if nucleated from a triple node of perfect dislocations. In this case, a twinning shear can be

accomplished when a displacement of $\frac{1}{6}\langle 121\rangle$ is applied successively to {111} twinning planes, which in practice is realized when the $\frac{1}{6}\langle 121\rangle$ Shockley partial dislocations are produced through the dissociation of $\frac{1}{2}\langle 101\rangle \text{ and } \frac{1}{3}\langle 111\rangle$ perfect dislocations. Therefore, the glide of the Shockley partials on the appropriate {111} planes would then produce many isolated intrinsic stacking faults, which overlap to produce a single or multi-layered macroscopic twins. However, other authors such as Priestner and Leslie [44] simply suppose that the stress concentration produced by intersecting slip is sufficient to nucleate twins homogeneously. As previously commented, the Pole mechanism has been equally applicable to fcc and bcc cubic lattices alike, but deformation twinning is difficult in single-phase fcc (such as Cu) metals due to the availability of multiple slip systems that are much easier to activate. For this reason, they usually require extreme conditions, such as shock and/or cryogenic temperatures, to generate the large stresses required to nucleate twins via pole mechanisms or dislocation dissociations. However, the low number of slip systems available in hcp metals makes twin propagation and growth very common and it is an important deformation mechanism responsible for the hardening and texture evolution when subjected to plastic deformation [45].

1.5. Multiple dislocation mechanism

This mechanism is based on the Frank–Read source concept of dislocation multiplication in a slip plane under shear stress. The Frank-Read source is an intragranular dislocation source where a dislocation segment lying on an active slip plane, and whose ends are pinned by the other parts of the dislocation lying outside the plane, bows out when subjected to stress [46]. When the critical stress is reached, this dislocation segment can generate dislocation loops thus resulting in dislocation multiplication.

The multiple twinning mechanism was first introduced by Muira and co-workers [47] and was expanded further in 1973 by Mahajan and Chin [48] to reflect what have been described as two co-planar model. Since then, multiple twins with various morphologies have been frequently observed in several metals including Cu, Al, Ni, Pd [49, 50] and other metals and their alloys. Considering that there are four equivalent {111} slip planes in an fcc metal, Muira and co-workers used the geometric relationships illustrated by the Thompson tetrahedron (Fig. 2a) to demonstrate that the multiple deformation twins are formed by glide of Shockley partials on planes in fcc materials. It has been observed that

the angle between any two slip planes is 70.53° and each edge of the tetrahedron represents the Burgers vector of a full dislocation, $\frac{1}{2}\langle 101\rangle$. Y.T. Zhu et. [51] demonstrated that unfolding the Thompson tetrahedron onto a flat surface yields a two-dimensional representation as shown in Fig. 2b. Thus, the four {111} slip planes (represented by four triangles) can be denoted as (a), (b), (c) and (d). Note that points a, b, c and d are at the centre of the triangles BCD, ACD, ABD, and ABC, respectively. The lines that link the centre of a triangle with its corners, e.g. Aβ, and δC, represent the Burgers vectors of partial dislocations on that slip plane. For simplicity, we define the direction of the Burgers vector as from the first letter to the second letter. For example, Aβ represents a vector from A to β, and AC from A to C. A dislocation whose Burgers vector links the centers of two slip planes is defined as a stair-rod dislocation (e.g. βδ). Thus, the multiple deformation twins can formed by glide of Shockley partials on planes (d) and (b). Orienting the Thompson tetrahedron (Fig. 2a) to make AC perpendicular to the page and using the axiom from Hirth and Lothe [52] (see Fig. 2b), a twin on the (d) plane can grow on the top twin boundary by the glide of the Cδ (or βδ or Aδ) partial to the right or the δC (or δβor δA) partial to the left. Similarly, the mechanism of twin nucleation in bcc crystals, with differing dislocation arrangements, has been studied for the past several decades, including the earliest by Cottrell and Bilby [43] and later by other authors [14, 53]. They discussed the mobility of twin boundaries in finite crystal structures and established the concept of concombined nucleation and growth model. By extending the theory of slip bands proposed by Frank and Read, they demonstrated the possibility of steady twin growth from plane to plane through a finite thickness of crystal as applied to body-centred and face-centred cubic lattices. However, many of current interesting theoretical alternatives and detailed microscopic observations in bcc crystals, including that of Sleeswyk et al. [54], have supported the fact that pre-existing twin boundaries become immobile in the presence of higher dislocation densities. They suggest that the “unusual elastic behavior” is probably related to the appearance/disappearance of micro twins [55]. Thus, they established that twins nucleate by dissociation of a perfect 1/2〈1 1 1〉 screw dislocation into three 1/6〈1 1 1〉 fractionals, which subsequently arrange on {112} plane [56]. Wang and Sehitoglu later observed that a key aspect is minimization of the total energy and the twinning stress during the twin nucleation process. They accounted for this using twinning energy landscape in the presence of interacting multiple twin dislocations and disregistry (i.e., magnitude of the displacement of the atoms from their perfect crystal positions)

profiles at the dislocation core to overcome successive energy barriers represented by the Generalized Planar Fault Energy (GPFE) curve. Fig. 3 shows the energy per unit surface γ (mJ/m^2) versus the normalized atomic displacement, u/b, where b is the Burgers vector. When continuous shear occurs along consecutive crystallographic (111) planes, then the GPFE is generated. A stacking fault upon shearing occurs along [121] direction of the perfect fcc lattice by one Burgers vector while the GPFE is created when shear on consecutive (111) planes occur along the same crystallographic orientation. As shear continues, a two-layer fault is generated upon displacement by 1b. For Co-33%Ni solid solution the energy barrier is 216 mJ/m^2 and the coherent twin boundary energy is 10 mJ/m^2. Further translation by another Burgers vector to a total displacement of 3b creates a twin nucleus and if the translation continues on successive layers above the twin nucleus, twin migration occur. In this proposition the GPFE curve was explored as the energy change per fault area to create successive twin layers. For hcp lattices, recent studies [14] suggest that the twinning mechanism deviates from the other classic dislocation-based nucleation mechanisms dislocations, because they are often compounded by the interaction with other conjugate twins. In contrast to metals with a body-centred cubic (bcc) or face-centred cubic (fcc) crystal structure, hcp structure metals have a large number of twinning planes, including $(10\bar{1}1)$, $(10\bar{1}2)$, $(10\bar{1}3)$, $(11\bar{1}3)$, $(10\bar{2}1)$, $(11\bar{2}3)$ and $(11\bar{2}4)$, although not all these are observed in the same metal [14, 57]. In addition, recently Wang et al. [58] suggested that twin nucleation in hexagonal materials is driven by local stress states and local atomistic configurations at grain boundaries (GBs). Thus, the traditional pole mechanism based on the gliding of a single twinning dislocation is not feasible for twin nucleation in hexagonal metals, because a single twinning dislocation does not exist alone in a perfect hcp structure. In addition, homogeneous nucleation of twins inside a grain is energetically and kinetically improbable because it involves a zonal dislocation with multiple atomic layers [59].

2. Effect of internal and external parameters on the critical stress for twinning

Nucleation is generally the critical event in twinning since for growth only a fraction of the nucleating stress is required, therefore, the critical event in twinning is, for most cases, nucleation [60]. If the external traction is very high, then the local stress will be high enough to nucleate twins as commented previously on the excellent overview of Christian

and Mahajan [14]. An accurate determination of the critical transformation twinning and deformation twinning stress parameter is crucial for the design of SMAs at various length scales [61, 62] and therefore the question that arises is, what is the stress required for twinning metals and its alloys?.

The stress required for twinning many SM metals and alloys depends on a number of internal and external parameters, including the chemical composition, grain size, temperature and strain rate. Some of these factors are difficult to separate, since they are strongly interdependent. Another major variable affecting the active twin modes is the crystal orientation–stress state relationship. The Schmid factor is a good predictor of the twinning system that will be active (i.e., twinning tends to occur in the orientation with maximum Schmid factor due to maximum twinning shear stress).

2.1. Internal parameters

2.1.1. Effect of composition

a) Ni–Ti and Ni–Ti based SMAs

The deformation behaviour of monoclinic and orthorhombic martensite in NiTi-based SMAs has been studied experimentally [63] and it shows that the flow response of the binary NiTi is primarily due to twinning of the monoclinic lattice at rather low stress levels (less than 20 MPa) [64]. Thus, since stress is an important criterion for the commencement of deformation twinning, an important consideration for these advanced alloys is the determination of the magnitude of the twinning stress.

In this regards, many authors have tried to understand and improve the functionality of Ni-Ti SMAS. Recently, K.M. Knowles and his colleagues studied the deformation mechanisms and the twinning evolution mechanism for the phase transformation from B2 to B19' in polycrystalline binary Ni-Ti SMA [65]. It was found that three types of twins are prevalent, namely, $\langle 11\bar{1} \rangle$ Type I, $\langle 011 \rangle$ Type II and $\langle 001 \rangle$ compound twins. Some types of twins are prevalent at very early stage of deformation, i.e., at low stress, while the activation of others occurs at more advanced stages of straining. The initial undeformed martensite primarily consists of Type I and Type II. This report further suggests that one variant of Type II twin, which is a major twinning mode frequently observed in NiTi SMAs, continues to grow in thickness at the expense of others in a process known as ‘‘detwinning”. The detwinning of $\langle 011 \rangle$ type II twin is achieved through the atomic shear along [011] direction of $(11\bar{1})$ plane. Yong Liu et al [66] observed that this twin response to applied stresses is responsible for various inelastic deformation processes as it can undergo deformation-

induced growth while the associated strains remain mostly recoverable. Knowles et al. [65] noted that at later stages of deformation, another compound twinning of (100) type is activated, in addition, $\langle 113 \rangle$ and $\langle 011 \rangle$ types of twins are also observed at later stages of martensite deformation, while (100), (001) and (201) compound twins coexist in the de-twinned variant. Another important difference between these two systems is their reflective symmetry. While the occurrence of (100) twin requires combined shear and shuffle, (001) twins can be created by shear alone.

At this last third stage, the martensite variant boundaries in most of the parent phase grains disappear. In other words, the variant coalescence has completed up to this stage by the growth of the most favourable variant with respect to the tensile axis. The presence of type (III) twins assist in increasing the ductility of the deformed martensite. Sehitoglu et al. [64] presented a computational comparison between the twinning energy landscapes for (001) and (100) modes and the results suggest that the (001) twinning is preferred due to its lower fault energy since the twin migration energy costs (i.e. the energy for displacing one layer from a pretwinned lattice) is 7.6 mJ m^{-2} and 41 mJ m^{-2} for (001) and (100) twins, respectively. However, the twinning shear magnitudes for both cases are 0.2385. It is worth mentioning that due to asymmetry of B19́ lattice, the equal amount of shearing requires overcoming different levels of energy barriers.

As previously discussed, the $\{20\bar{1}\}$ type twinning is another twinning mode that can occur in conjunction with the (001) compound twinning. According to Zhang et al. [67], this $\{20\bar{1}\}$ compound type twinning mode is typically observed beyond the stress plateau at a strain level >3%. A comparison of the energy barriers via combined shear and shuffle during the (001) and (100) twin growth show that $(20\bar{1})$ $[\bar{1}02]$ twinning possess a higher magnitude, which was attributed to the non-cubic nature, i.e., lower symmetry, of the B19́ martensite lattice [64]. As this DFT calculations confirmed, a shear magnitude of 0.338 Pa accompanied by atomic shuffles gives rise to an energetically stable twin embryo. The low shear magnitude needed for twinning reduces the possibility of slip nucleation before twinning. Dislocation activities can also accompany the deformation at this stage, to preserve the shape memory effects, which entails that twinning remains the primary deformation mechanism while minimizing slip.

It is well known that current SMAs are limited to temperatures below 100°C. Moreover, when subjected to thermomechanical processes, it can result in stable shape memory or superelastic behaviour and the transformation temperatures are further

reduced [68]. The development of high-temperature shape memory alloys with potential industrial applications have attracted much attention from researchers [69], [70] and [71]. For NiTi at temperatures above 100°C, the lowering of the slip stress and other recovery mechanisms can induce plastic deformation. One of the most promising high-temperature shape memory materials is NiTi with ternary or quaternary additions [72]. There have been notable recent developments in the NiTi-X (X = Hf, Zr, Pd, Cu, Hf, Fe and Au) systems, and it has been demonstrated that stable cyclic actuation up to 400 °C is possible [73]. Addition of a third element (i.e., ternary alloys) into Ni-Ti can have different effects. For example, addition of 10 at. % Pd results in a notable increase of transformation temperatures (TTs) [74]. Sehitoglu and Vítek et al. [75] have found that Ni-Ti-Hf alloys are more practical for engineering applications than Ni-Ti, primarily due to high transformation temperatures, good thermal stability and lower price. Specifically, Ni-Ti-Hf alloys with up to 25 at. % Hf undergo a B2-to-B19′ martensitic transformation similar to that of Ni-Ti [76] while Hf or Zr content of 10 at. % leads to a significant increase in the TTs [69]. It was reported that the corresponding twin and slip stresses for Ni-Ti-Hf martensites undergo twinning at lower stress levels than the slip stresses. Both slip and twinning stresses for martensite Ni-Ti-Hf increase as the Hf content becomes larger. Compared to the slip stress of 36 MPa in martensitic Ni-Ti, the slip stress in martensite Ni-Ti-Hf varies from 286 to 556 MPa, while the twinning stress in martensite Ni-Ti-Hf varies from 161 to 291 MPa, much higher than the corresponding value of 20 MPa for Ni-Ti.

The precise shuffles within the orthorhombic martensite crystal structures for 25 at. % Hf were established via simulations by Wang and Sehitoglu [64]. They observed that ternary alloys, such Ni-Ti-Hf, have different atomic arrangement compared to the binary Ni-Ti and thus their shuffle magnitudes are different than those of Ni-Ti. The shuffle magnitude of Ni-Ti-Hf is 0.42 Å, which corresponds to the shuffle mode (010)[001], while for 0.14 Å the shuffle mode is (001)[100]. These values are different from the corresponding shuffles in Ni-Ti of 0.46 Å [43] and 0.17 Å [51] for (0 1 0)[0 0 1] and (0 0 1)[1 0 0], respectively. Depending on the martensitic structure, the twinning system in Ni-Ti-Hf can be different. In B19′ monoclinic Ni-Ti-Hf, the twinning system is (001)[100]. However, the (001) is a plane of symmetry in B19 orthorhombic structure and thus it is not a twin plane. In B19 orthorhombic Ni-Ti-Hf, the twinning system is $(011)[01\bar{1}]$. In both B19′ Ni-Ti and B19’ Ni-Ti-Hf the slip system is (001)[100]. Altogether, Ni-Ti-Hf SMAs offer considerable promise for high temperature applications, especially in aerospace and electronics industries.

This is also similar to the observations for Ni-Ti-Cu SMA, for which DFT studies focused on lattice structure and stability have also emerged [77]. In addition to a decline in lattice constants with increasing Cu content, it is found that Cu alters the transformation pathway, whereby, depending on Cu content, intermediate B19 phase can be prevalent in the microstructure. With Cu content <7.5 at. %, the transformation occurs from B2 to B19'; for Cu between 7.5 at. % and 15 at. %, the path becomes B2→B19→B19́ and B2 →B19 for Cu concentration higher than 15 at. %. Gou et al. [78] further corroborated that the addition of Cu has the effect of reducing the monoclinic angle of the martensite phase. They noted the increasing instability (manifested in terms of rising free energy) of monoclinic B19́ structure with increasing Cu addition. Specifically, a threshold range was predicted, noting that for 0 at. % < Cu < 18.75 at. % martensite is monoclinic whereas at 20 at. % it becomes orthorhombic. Altogether, these findings rationalize the predominance of the B19 phase (having orthorhombic structure) with high Cu content in the experimental observations.

For NiTi SMAs, dislocation glide plays a key role in accommodating the plastic deformation, with the three operational twinning variants but deformation twinning can also occur at higher stresses on the {114}<112> system [79]. However, because the CRSS for twinning is near 200 MPa in these alloys, the slip-mediated plastic flow dominates for the strain ranges studied except along the [001] compression direction of the sample. For [001] direction, the alloy exhibits deformation twinning, thus imparting additional ductility to Ni-Ti-Cu alloy in the austenitic regime. This twinning mode have also been are noted in other alloy systems, namely Ti-Ni-Al, Fe-Ni-C, Fe-Pd, In-Tl, Ni-Al, Ni-Mn, Ni2-Mn-Ga.

b) Fe and Fe- based shape memory alloys

Martensitic transformation was first found in ferrous alloys, which are among the most important materials in modern engineering. There is a number of Fe and Fe based SMAs that can be classified into four groups, as following [80] fcc–bcc (Fe–Ni), fcc–bct (Fe–Pt, Fe–Ni–Co–Ti, Fe–Ni–C, Fe–Ni–Nb) transformation from fcc austenite to bct (body-centered tetragonal) martensite, fcc–fct (Fe–Pt, Fe–Pd) transformation from fcc austenite to fct (face-centered tetragonal) martensite and fcc–hcp (Fe–Mn–Si, Fe–Cr–Ni–Mn–Si, Fe–Mn–Si).

Iron (Fe) and iron based alloys have been developed to exhibit twin-induced plasticity (TWIP) and strengthening. The synergistic effects of the interaction between deformation twins and dislocations in TWIP steel have rendered the development of high

performance steels [17]. It is now possible to defy the conventional strength-ductility trade-off by modification of the composition, processing, and microstructure of structural metals and alloys. This peculiar simultaneous enhancement of ductility and strength in TWIP steels is attributed to the high work-hardening rate associated with multiplicative interactions between deformation twins and dislocations [81].

Fe-based SMAs such as Fe–Mn–Si, Fe-Ni-C, and Fe-Ni-Co-T and Fe-Mn-Si-Cr-Ni were first discovered and developed in Japan [82] and over the years different elements have been added to tune the performance of the parent Fe-based SMA. For example, Cr and Ni are frequently added to provide high corrosive-resistance. Tanaka et al. [83] reported a huge superelastic strain >13% at room temperature in an Fe-28Ni-17Co-11.5Al-2.5Ta-0.05B at. % steel, and Omori et al. [84] attained a superelasticity of >6% in an Fe-34Mn-15Al-7.5Ni at. % steel with a mean grain size of ~3.8 mm having a bamboo structure. These alloys have advantages in commercial production due to their inexpensive constituent elements and availability of the mass-production facilities that are readily used for the production of stainless steels. Fe based SMAs have received considerable attention in the past two decades due to their low cost, good workability, good machinability and good weldability. The shape memory effect is attributed to the stress-induced martensite transformation from a parent γ phase (fcc) to an ε phase (hcp). The critical stress for twin nucleation in many Fe based polycrystals, with differing dislocation arrangements, has been studied for the past several decades [14] [53] and many of these results (Table 1) reveal that the critical twinning stress for bcc Fe depends on the twin nucleation mechanism. It is evident from Table 1, that the results predicted by the different mechanisms are much higher than the experimental value of 170 MPa for Fe. Ojha et al [85] estimates that the errors leading to high twinning stress are most likely due to incomplete description of the energetics associated with twinning and insufficient geometrical consideration of the fractional dislocations. Recently, Ojha et al. [86] relied only on parameters that are obtained through atomistic calculations to minimize the total energy to predict the twinning stress, thus excluding the need for any empirical constant. The critical stress obtained from Molecular Dynamic (MD) simulations was validated by means of precise measurements of the onset of twinning in bcc Fe–50Cr at. % single crystals via transmission electron microscopy techniques along with digital image correlation [86]. The validity of the model was confirmed by predicting the twinning stress for pure metals (Fe, V, Nb, Ta, Mo and W) and alloys, (Fe–25Ni, Fe–3Si and Fe–3V at. % alloys) and the results compared with experiments from the literature to show general

applicability. The energy landscape associated with twinning provides a better twin migration stress in relation to the twin nucleation stress with a ratio of 0.5–0.8 depending on the resultant residual burgers vector and the intersection types in Fe and Fe based alloys. The theoretical (ideal) twinning stress calculated from the generalized plane fault energy (GPFE) curves with respect to the shear displacement can be written as $\tau = \pi\gamma\Gamma BM/b$, where $\gamma\Gamma BM$ is the difference between the unstable twin fault energy, γ_{ut}, and the stable twin stacking fault energy, $2\gamma_{tsf}$. The Peierls stress (i.e., the minimum shear stress required to move a dislocation) for twinning the element Mo by using their proposed equation is 448 MPa, which agrees with the experiments (472 MPa), but it is lower than the theoretical stress of 3270 MPa. Nonetheless, other variables such as shear modulus and stacking fault energy value also determine the twinning stress. For example, in the case of Fe–3 at. % Si, the total separation distance of 76 Å is much lower compared to all other bcc crystals considered, yet the twinning stress of 298 MPa is higher than that of Fe, V, Nb, Ta and Fe–3V at. %. This is attributed to the lower shear modulus of Fe–3Si at.% compared to that of pure Fe metals (see Table 2) and to the considerably higher stacking fault energy value (241 mJ m^{-2}). The theoretical results are compared with those obtained from the experiments as listed in Table 2, while the normalized plot shown in Fig. 6 summarizes the twinning stress for a number of bcc metals and alloys considered.

c) Cu and Cu-based shape memory alloys

Although Cu based SMAs do not exhibit a shape memory behaviour as good as that of Ni–Ti alloys, they are of interest not only because they are cheaper and easier to fabricate but also because they have superior performance than Fe based SMAs. The cost-effectiveness of Cu based SMAs alloys is not only attributed to the lower cost of Cu compared to Ti, but also because they are not very reactive and can therefore be easily produced using ordinary liquid and powder metallurgy routes [87]. On rapid cooling from high temperatures, the β phase in Cu SMAs undergoes a martensitic transformation. When quenched from the β state, it transforms into an fcc type of disordered martensite. Commonly, the bcc phase is not stable at moderate temperatures, but can be retained by means of a suitable cooling rate. During this cooling, the system becomes configurationally ordered and can strongly modify the vibrational characteristics of the bcc lattice and therefore have an influence on the phase stability of the system.

The shape memory properties of Cu-based SMAs are quite sensitive to the alloying elements used to adjust the martensitic transformation temperature of the alloy. This enables to tune the performance of austenite (i.e., B2 CuZr) and thus to improve the plastic deformability. For this reason it is important to understand the influence of deformation-twins (DTs) in Cu-based shape memory alloys, which can explain the interest that it has attracted over the last years. For example, S. Alkan et al. [88] observed that the low transformation stress for super-elasticity relative to slip stress in CuZnAl presents a unique opportunity for engineering applications. The experimental results show that the critical resolved shear stress (CRSS) for austenite to slip is in excess of 200 MPa in CuZnAl alloy, which far exceeds the transformation stress level varying from 25 MPa to 60 MPa depending on the crystal orientation. Introduction of crystallographic disorder in simulations resulted in an increase of the transformation energy barrier from 68 to 86-96 mJ/m^2 as well as increasing the critical transformation stress from 25 MPa to 33 MPa for the sample under tension.

Deformation twinning has been studied over the years for different Cu and Cu based shape memory alloys such as Cu-Al [89], Cu-Mn [90] and Cu-Zn [91]. Recently, Liu et al. [89] observed that deformation-twinning is a dominant mechanism in Cu-Al alloys with high Al content, exhibiting synchronous improvement of strength and plasticity (SISP), as in TWIP steels. The authors reported a simultaneous increase in the strength and plasticity of Cu-Al alloys, named as “TWIP copper alloys”, following the concept of TWIP steels. The pronounced improvement of both strength and plasticity, in TWIP copper alloys and TWIP steels, was due to constructive interaction between deformation-twins and dislocations. The SISP in Cu-Al alloys was attributed to the change in slip-mode and increased density of deformation-twins, associated with the decrease in the SFE. The authors also studied the effect of Mn content, from 5 to 20 at. %, on the performance of Cu-Mn alloys. They observed that as the Mn content increases, the alloys exhibited higher SFEs (close to that of pure Cu) and displayed dislocation-cells to planar-slip structures. The interaction between these dislocation slip structures with deformation-twins enhances the strain-hardenability, causing an improved strength and ductility. The enhanced deformation-twining in both Cu-15 at. % Mn and Cu-20 at. % Mn alloys, can improve the strength by increasing the work-hardening rate through the effect of TWIP, similar to TWIP steels, TWIP Cu-Al alloys and Cu-Zn alloys.

d) Other alloys that exhibit twinning

Titanium: Ti–Ni shape memory alloys are increasingly important for multiple applications such as guidewires and stents for medical device tools [92]. The B19′ structure present in Ni-Ti martensite is very unique [93] since it has many twinning modes with reasonably small twinning shear and gives the lowest energy by first-principles calculations [94], which can explain why Ti–Ni alloys exhibit such good shape memory behaviour. However, due to the potential hypersensitivity and toxicity of Ni, Ni-free shape memory alloys are desired [95]. Metastable β-type Ti alloys, such as Ti–Nb, Ti-Nb-Zr, Ti-Mo, Ti-Nb-Sn, Ti–Ta, exhibit shape-memory effect and superelasticity due to thermoelastic and stress-induced martensitic transformations [96]. These alloying transition elements exhibit complete miscibility at high temperatures but transform from bcc to martensite upon cooling. The structures of the martensite is dependent on solute contents. In other words, when the solute content is low, the martensite has a hcp structure, while at higher content, the structure is orthorhombic [97].

A. Ojha, et al [98] carried out first-principles calculations for Ti–Ta alloys and they studied the effect of Nb and Ta additions on (i) the critical resolved shear stress (CRSS) for the β →α″ transformation, (ii) the CRSS for austenite slip, and (iii) the CRSS for twin nucleation in martensite (α″ phase). Their calculations showed that an increase in Ta content from 0 to 37.5 at.% increases the CRSS for austenite and martensite slip by more than 90 %, while the twinning stress increases by 25 %, and the transformation stress by 40 %. Overall, as the content in Ta increases, the difference between martensite/austenite slip and the transformation/twinning stress decreases. Although, this is in contrast to other experiments [99] and [96] on binary Ti–Ta alloys, which have shown that a decrease in Nb content increases the critical stress to induce martensitic transformation. The result indicate that Ti–25Nb alloy exhibits shape memory behaviour with complete strain recovery of approximately 2.2 %. The critical twinning stress of Ti–25Nb is 72 MPa, which is lower than the CRSS of martensite slip by 156 MPa and hence the alloy exhibits complete strain recovery without undergoing any plasticity [99] It is also possible that (i) the incomplete description of the energetics associated with twinning and (ii) the insufficient geometrical consideration of the fractional dislocations may have contributed to the observed inconsistencies.

Magnesium: Twinning is an important deformation mechanism for Mg and Mg alloys due to the small number of slip systems available in hexagonal crystals. Over the years different Mg alloys with enhanced performance have been developed. For example,

Ogawa et al. [100] reported a new type of lightweight SMA made from magnesium and scandium, which has comparable properties to known SMAs but with significantly lower density, of about 2 grams per cubic centimetre, which is one-third less than that of Ti-Ni SMAs, and therefore it is of interest for lightweight applications. The alloy also shows superelasticity of 4.4 % at –150°C and shape recovery upon heating due to the reversible martensitic transformation. A magnesium-scandium alloy rich in Mg (Mg ~ 80 at. %) with bcc structure [101], designated as β phase, was developed to keep the structure at a higher temperature range. Other Mg-Sc alloys contain both β and α phases [102] with both a high ultimate tensile strength of 280 MPa and a large tensile elongation of ~30% at RT. During deformation, this β-type Mg-Sc alloy shows age hardening at ~200°C due to the formation of fine hcp (α) needles and/or plates in a β matrix and exhibits an extremely high hardness of ~230 HV.

2.1.2. Effect of grain size

As previously commented, there are two main deformation mechanisms, slip and twinning, and both of them depend on the grain size. According to experimental results first reported in the literature by Armstrong et al. [103], smaller grain size impedes deformation twinning while when the grain size is larger the twinning stress depends on grain dimensions but not on the crystal structure. These findings have been observed in different metals and alloys, such as copper [104], brass [105], titanium [106], magnesium [107] and twin-induced plasticity (TWIP) steels [108]. The landmark paper by Meyers et al. [109] summarizes the Hall–Petch slopes for both perfect dislocation slip and twinning in a number of coarse-grained metals with fcc (body-centered cubic), body-centered cubic (bcc) and hexagonal-close-pack (hcp) crystal structures. Their result indicates that twinning subdivides the grains and therefore increases the barriers to slip, thus increasing the work-hardening rate. There are, however, some contradictory conclusions with regards to the effect of grain size on twinning in the literature. For instance, it is unclear why deformation twins are observed only in some grains in low-SFE alloys during tension, while other grains of similar size lack deformation twins. We suggest that this may be caused by different crystalline orientations (i.e., Schmidt factor). The influence of the grain size on the twinning stress enables to design shape memory alloys with tuned behaviour for engineering applications. The effect of the grain size depends on the type of alloy system:

a) Ni-Ti and Ni-Ti based SMAs

Nishida et al. [110] studied the effect of grain size of B2 parent phase on the twinning modes of B19' martensite in a NiTi shape memory alloy. The result is consistent with the previous observation by Armstrong in a NiTi shape memory alloy [103], when they used cold-rolling and subsequent annealing to control the grain size of parent phase from submicrons to several ten microns. In this study, (001) compound twins were dominantly observed in grains of less than 4 μm size, but did not give a solution when grains are larger than 4 μm. C. Chluba et al. [111] studied the influence of the grain size on the twinning stress and other properties by using two TiNiCuCo samples prepared by sputter deposition and sequential annealing. These samples had similar crystallographic compatibility and precipitate content but different grain sizes. After exposure of the samples to thermal and superelastic cycling, the grain size was observed to be the determining factor responsible for the increase in the yield strength. A larger grain size decreases the twinning and improves the shape memory and superelastic cycling behaviour. The peak stress observed at the start of the superelastic plateau is assumed to be the energy barrier for the stress-induced martensite transformation. Compared with the nucleation stress, the actual movement of the martensitic transformation interface during the transformation is 50 MPa lower. Therefore, for the investigated TiNiCuCo compositions, grain refinement results in a higher yield strength and a better resistance to dislocation nucleation and movement. In agreement with the above results, an investigation from synchrotron experiments conducted on TiNiCuCo alloys at different temperatures, further indicate that during the transformation of samples deformed at 700°C, the crystallographic plane changed from 3.012 Å ((100) B2) to 2.886 Å ((100) B19'). However, for the samples deformed at 600°C from 250 MPa to 330 MPa, the planes distances increased from 3.005 Å ((100) B2) to 2.893 Å ((100) B19). In effect, the lattice misfit (100) B2 / (100) B19' of 3.8% for the sample annealed at 600°C is smaller compared with 4.3% for the sample annealed at 700°C [91].

b) Fe and Fe-based SMAs

In body-centred cubic metals and alloys, such as pure Fe, twinning takes place at low temperature because the stress for dislocation slip increases sharply with decreasing temperature, which makes twinning become a favourable deformation mode [112]. Twinning is also commonly detected in Fe alloys exhibiting SM behaviour, such as TWIP steels. Deformation twins are responsible for the outstanding mechanical properties of TWIP steel as reported by Gutierrez et al [113]. TWIP steel samples of Fe–22Mn–0.6C wt.

% with average grain sizes of 3 μm and 50 μm were deformed in tension at room temperature to different samples to investigate the effect of grain size and grain orientation on deformation twinning stress by observing the microstructure by electron channelling contrast imaging (ECCI) and electron backscatter diffraction (EBSD). They observed that grain refinement within the micrometre range does not suppress deformation twinning for the present TWIP steel when deformed in tension at room temperature. Deformation twinning becomes more difficult as the average grain size decreases, but even for sizes as small as 3 μm, twinning is not completely suppressed. Grain refinement produces a strong decrease in the twin area, from 0.2 % for an average grain size of 5 μm to 0.1 % when the average grain size is 3 μm for 0.3 logarithmic strain [113]. Deformation twinning is reported to be responsible for the outstanding mechanical properties of TWIP steel. It is therefore feasible to tailor the mechanical properties of Fe–22Mn–0.6C wt.% TWIP steels through grain refinement within the micrometre range, and, hence, to inhibit twinning.

To provide a good estimation of the grain size effect within the micrometre range on the twinning stress, Hall–Petch relations has been used by different authors. In one approach the following Hall–Petch type relation was proposed [109]:

$$\tau_{tw} = \frac{\gamma}{b} + \frac{Gb}{D} \qquad (12)$$

where, τ_{tw} is the critical resolved shear stress for twining, γ the SFE, D the grain size, G the shear modulus and b is the Burgers vector. This equation only describes the stress for nucleation of twins on boundaries. The growth of a twin in a homogeneous, single crystal matrix, however, is not considered. This growth stress is in principle the stress to drive the partial dislocations away from each other and may therefore be given by γ/b [114]. However, this cannot not be generalized to other TWIP steel systems. For instance, Ueji et al. [115] noted a strong reduction in twinning activity in a Fe–31Mn–3.0Al–3.0Si wt. % TWIP steel after similar grain refinement (average grain size of 1.8 μm) using also similar deformation conditions. The only difference is that the stacking fault energy (SFE) in Fe–31Mn–3.0 Al–3.0 Si wt.% TWIP steel is larger than that in Fe–22Mn–0.6C wt. % TWIP steel (around 40 mJ/m^2 against 22 mJ/m^2), respectively [116]. Thus, the stacking fault energy, determined by chemical composition, plays a key role in the twinning behaviour of TWIP steels. Therefore, for a better understanding of twinning in TWIP steels, both parameters, stacking fault energy and grain size must be considered.

Grain coarsening may have a positive effect on the recovery strain of Fe-Mn-Si based SMAs, however that comes with compromising the strength due to the relationship between grain size, annealing twins and shape memory effect. This complex relationship is therefore of interest to investigate the effect of the grain size on the Shape Memory Effect (SME) in terms of transformation temperature and recovery strain. There is, however, conflict in the findings of different researchers. For example, Tan et al [117] found that SME decreases with the increase of grain size, i.e., within the range 10-60 μm, because of the effect of the density of perfect dislocation in coarser grains generated during deformation is significantly higher compared to that in the finer grains [117]. On the other hand, Jee et al. reported an improvement in SME with increasing grain size, which is attributed to the ease of the transformation upon deformation [118]. Interestingly, Wan et al. reported that an increase of grain size, as long as it is below 10 μm, leads to the increase of SME, however, it decreases when the grain size exceeds 10 μm. This is attributed to the fact that grain refinement is only effective at a certain region of grain size and for Fe-28Mn-6Si-4Cr-0.2C wt. % alloy, 10 μm is considered the critical size [119]. In another study conducted by Murakami et al. [120], ranging grain size between 20-200 μm was reported to have no clear effect on SME values [121]. Based on the outcome of the different researches mentioned above, an investigation was conducted [122] where Fe–21.63Mn–5.60Si–9.32Cr–5.38Ni at. % alloy was heat treated at different temperatures and times, 1273 K for 5 min, 1373 K for 5 min, 1373 K for 120 min and 1423 K for 120 min, thus resulting in different mean grain sizes of 48.9 μm, 78.4 μm, 180.3 μm, and 253.6 μm respectively. It was found that for Fe–21.63Mn–5.60Si–9.32Cr–5.38Ni alloy, the grain size reduction causes the SME to decline. This is caused by the fact that grain refinement lowers the ability to suppress plastic deformation and facilitate the stress-induced ε martensite transformation (SIEM). However, the authors also observed [102] that grain refinement increases the density of annealing twins and grain boundaries and raises their constraint effects on martensitic transformation.

c) Cu- and Cu-based SMAs

In face-centred cubic (fcc) metals, deformation twinning is observed, especially when the stacking fault energy (SFE) is low to medium, after thermo-mechanical treatment involving annealing and cold working [122-125]. For high SFE elements, such as Ni and Al, twinning is rarely observed [35]. For Cu single crystals, a metal with medium–high SFE, Blewitt et al. [126] reported that deformation twinning occurred when it was subjected to

tension at 4.2 MPa and 77.3 K. At the same time, the experimental observations have also demonstrated that deformation twinning in coarse grained Cu or Ni took place only after sufficient strain hardening has occurred [127]. For those materials with relatively high SFE, like Cu (aprox. 39 erg/cm^{-2}), El-Danaf et al. [128] detected that either a certain critical amount of dislocation density, a very low temperature and/or a high strain rate (~10^3 s^{-1}) are required for the nucleation of deformation twins and suppress dislocation-slip processes. It was observed that deformation twinning takes place in polycrystalline Cu with grain sizes varying from micrometres to nanometres or in ultrafine and NC grains via partial dislocation emission from GBs and GB junctions.

Grain size, among other factors such as SFE, influence the formation of annealing twins [129]. The relationship between the density of annealing twins, the SFE and the grain size of Cu-Al and Cu-Zn where found to be inversely proportional [122]. Similarly, El-Danaf et al. used pure (99.97%) polycrystalline Cu rods annealed at 600°C for 40 min for the ECAP for: (a) 1, (b) 8 and (c) 24 passes, respectively [128] to study the effect of grain size on deformation twinning stress. With an increase in the pressing passes, ultrafine grains were formed via the processes of grain subdivision, evolving dislocation accumulation, tangling and rearrangement. Other studies [130] have shown that deformation twinning can take place in ultrafine and NC grains via partial dislocation emission from GBs and GB junctions. Therefore, C.X. Huang et al. [130] concluded that deformation twinning takes place in coarse Cu grains mainly in shear bands and their intersections, since these places undergo severe plastic deformation as a result of localized plastic deformation effect. Hence, twinning triggered in these sites is caused by very high local stresses up to the level of the critical twinning stress. However, deformation twins in UFG- and NC-Cu (i.e., ultrafine and nanocrystalline Cu) nucleate from GBs and GB junctions and grow via successively partial dislocation emission from the adjacent (111) slip plane. At grain sizes of several hundred nanometres, the twinning mechanism transforms from the pole mechanism in the CG case to partial dislocation emission from GBs and GB junctions.

However, Meyers et al. [109] observed that shock compression at 35 GPa produced profuse deformation twins in Cu samples with average grain sizes of 117 and 315 μm but virtually no twin in Cu samples with an average grain size of 9 μm. For this reason a conflict still exist in the understanding of the phenomenon with regards to Cu and Cu based alloys. The effect of variation of grain size (from 1 μm to smaller than 100 nm) on deformation twinning in fcc, bcc and hcp was studied experimentally by Zhu et al. [131]. It is known for coarse grains that the critical stress for dislocation slip can be described by Hall-Petch

relationship ($\sigma_s = \sigma_0 + k_s d^{-1/2}$) [131, 132], where the parameters are, d grain size, σ_0 a constant and k_s the Hall-Petch slope for dislocation slip. Similarly, experimental results show that the critical stress for twinning also follow Hall-Petch relationship ($\sigma_T = \sigma_{0'} + k_T d^{-1/2}$) where k_T: Hall-Petch slope for twinning. Table 3 shows the k_s and k_T slopes and their ratio (and k_T/k_s) for different metals and alloys. While steel, Zr and Cu have large slope values, those for other elements such as Ti and alloys such as Cu-6 wt. % Sn are very small.

Figure 7 illustrates a schematic of the critical stress required to activate deformation twinning depending on the grain size [131]. Beyond a critical grain size for which the twinning stress is maximum, increasing the grain size tends to continuously decrease the twinning stress and this is valid for fcc, bcc and hcp structures [109]. However, below the critical grain size, for nano grains with fcc structure, the twinning stress tends to rapidly decrease as the grain size decreases [131, 133, 134]. Figure 8 shows a representation of the evolution of the twinning stress and stress for dislocation slip as a function of the grain size following the Hall-Petch equation (i.e., the stress increases with a decrease of the grain size). The slope, and therefore the grain size effect, is larger for twinning (k_T) than for dislocation slip (k_s) as shown in Fig. 8 and listed in Table 3 for different materials with fcc, bcc and hcp structure.

d) Other alloys that exhibit twinning

Deformation twinning is a common and important mechanism for plastic deformation in hexagonal close packed metals, such as Ti and Mg. The effect of grain size on microstructure evolution are also pronounced for other polycrystalline hexagonal close packed metals with low-symmetry crystal lattice. Therefore, the two main deformation mechanisms, slip and twinning, are associated with the different dependencies on grain size of critical resolved shear stress for slip and twinning.

S.V. Zherebtsov et al. [106] have previously found that the contribution of twinning decreases with a decrease in grain size and below certain grain size twinning was not observed. This was demonstrated through microstructure evolution observations in commercial-purity titanium (CP Ti) of various initial grain sizes 1, 7, 15 and 30 μm during plane-strain multipass rolling to a true thickness strain of 2.66 at 293 K (20°C). The effect of grain size on twinning in titanium was discussed in the context of a declination model and it was established that the degree of deformation twinning is strongly dependent on grain size. It was found that twinning is rare for 1 μm grain size but for all grain sizes larger than 15 μm, the occurrence of twinning reached similar maximum value. Concurrently, the

propensity for twinning enhanced the kinetics of microstructure refinement upon rolling, particularly for the initially coarse-grain materials. Due to the extensive twinning-induced microstructure refinement, rolling of coarse-grain (15 μm) CP Ti to a true thickness strain of 2.66 resulted in the formation of an ultrafine microstructure with a grain/sub grain size of 200-300 nm, a value similar to that attained for the initially micrometre-scale microstructure. At room temperature, for instance, this critical grain size has been found to be 0.9 μm for CP Ti [135] and 1 μm for Ti-5Al [136]. Thus, they concluded that twinning large imposed strains could affect the nature and kinetics of the formation of ultrafine microstructures. Similarly, the grain size effect was demonstrated in many other alloys, including brass. For instance, El-Danaf et al. [128] observed that 70/30 brass can show much greater twin density with increasing the grain size of about 250 μm than in samples with smaller grain sizes of 9 and 30 μm.

2.2. External parameters

2.2.1. Effect of temperature/strain rate

For the past fifty years, the relevance of the effect of temperature sensitivity on twinning stress has attracted intense debate and diverging results and opinions abound in the literature. For instance, some researchers, such as, Bell and Cahn [31] have shown evidence of clear temperature insensitivity in some polycrystalline materials and sensitivity in monocrystals and vice versa. However, according to other authors like Mahajan and Williams [137], the twinning stress depends on the specific structure of the crystalline phase. For example, bcc metals seem to have a negative dependence of twinning stress on temperature, while fcc metals have a slightly positive temperature sensitivity. Reed-Hill [138] provided further evidence based on the work on bcc Fe_3Be by Bolling and Richman [139], and they concluded that whenever the deformation proceeds primarily by twinning, the flow stress tends to have a positive temperature dependence and a negative strain rate dependence. However, there are reports of a gradual decrease in the twinning stress with increasing temperature for fcc metals, including that of Bolling and Richman, and of Koester and Speidel [140]. Other authors, such as Meyers et al. [109], observed that there are some alloys including Fe-25Ni at. %, Fe-3.3Si, Fe-2.5Si, Cu-20Zn and Ag-4In wt. % check for which the critical stress for twinning is either temperature independent or has a very low temperature dependence. Figure 9 shows a temperature insensitive compilation of twinning stress vs temperature for a number of metals (both mono and polycrystals) [109]. Fe-based alloys exhibit higher twinning shear stress than Cu or Ag-based alloys but

they exhibit similar temperature range for which the twinning stress is insensitive. The effect of temperature/strain rate on the twinning shear stress has been reported for NiTi SE508 shape memory alloy tested under compression over strain rates of 10^{-3}–7.5×10^{2} s^{-1}, i.e., quasi-static and dynamic loading, by Chen et al (2001) [141]. For this alloy, the value of A_f ranges from 5 to 18°C and therefore, when tested at room temperature, i.e., beyond 18°C, within the commented strain rate range, the material exhibits superelasticity, stress-induced martensitic transformation and variation of the work-hardening rate. When the alloy is tested in compression upon quasi-static conditions, (10^{-3} s^{-1}) there is a transition from linearly elastic to superelastic behaviour at a stress of approximately 550 MPa, thus suggesting that the alloy exhibits stress-induced martensitic transformation. When unloading, the stress-strain curves return to the origin and therefore hysteresis loops are completely closed. At dynamic loads, there is a residual deformation upon unloading at the beginning but tends to slowly recover its length. Similar tests were conducted by S. Nemat-Nasser [142] on a 50.4Ni-49.6Ti at. % alloy at 296 K but within the following wider strain rate range:

• **Dynamic compression tests** (10^{2} to beyond 10^{3} s^{-1}) using a split Hopkinson pressure bar with a pulse shaper. The work-hardening, defined as the slope of the stress-strain curve, tends to increase with increasing volume fraction of stress-induced martensite. The hardening was reported to be strain rate dependent in the range of the studied strain rates (330 to 1,080 s^{-1}). Two factors where considered by these authors [142] when analysing the stress-induced martensitic transformation. First, this transformation is an exothermic process and therefore results in an increase in the temperature of the sample upon loading. Second, the heat generated remains within the sample when tested at high strain rates. This temperature increase has an effect on the critical stress for the stress-induced martensitic transformation according to the Clausius-Clapeyron equation [143]. The temperature rise upon loading at high strain rates not only depends on the previously commented latent heat of transformation from austenite into martensite but also on the strain rate itself due to the deformation process since for high values of the strain rate the deformation is essentially adiabatic. The total increase of temperature (ΔT) can therefore be written as $\Delta T = \Delta T_d + \Delta T_L$ where ΔT_L corresponds to the latent heat and ΔT_d corresponds to the heating upon deformation as following:

$$\Delta T_d = (\beta/\rho C)\sigma d\varepsilon \qquad (1)$$

Where ρ is the mass density (ρ = 6450 Kg/m^3 for the NiTi alloy); β corresponds to the fraction of the work actually converted to heat ($\beta \approx 1$) [144], and C is the average heat capacity of the sample (C= 500 J/KgK).

• **Low strain rate tests** (10^{-4} to 1 s^{-1}) using an Instron in compression. For NiTi alloys tested at room temperature at a maximum strain within the superelastic range [142], the transition stress (Fig. 10a) and the work hardening rate (Fig. 10b) were observed to increase as the strain rate increases (10^{-4} to 1 s^{-1}) and therefore it is strain rate dependent. Fig. 10b shows that for up to about 1s^{-1} the work-hardening rate of the stress-induced martensite formation increases linearly with an increase in the strain rate. For strain rate from 1s^{-1} up to 1000 s^{-1} it remains practically constant but increases with increasing strain rate beyond 1000 s^{-1}. This behaviour suggests a transition stress from austenite to martensite at about 1000 s^{-1} so that at lower strain rates the interfacial motion of martensite is dominated by thermally-activated motion of dislocations while at higher strain rates there is an interfacial drag effect. Liu et al. [145] also studied the effect of the strain rate on twinning by performing compression tests of NiTi SMA at strain rate up to 3000 s^{-1} by using a Kolsky bar. They observed that the deformation mechanism is different in tension and compression since in compression it is mainly associated with dislocations generations while in tension it is attributed to a detwinning process. The authors also investigated the behaviour in tension at strain rates from 0.002 up to 300 s^{-1} [146]. The deformation mechanism was reported to be insensitive to the strain rate at this strain rate interval and they detected the presence of a stress plateau associated with the martensite detwinning process even at high strain rates.

a) NiTi and Ni-Ti based alloys

The deformation behaviour of hexagonal close-packed (hcp) metallic materials, including Ti, Zr , Mg and hcp SMAs is complicated due to the activation of both slip systems and twinning systems [136]. In the past several decades, the occurrence of deformation twinning in hcp metallic materials under low speed deformation rate has been widely reported [137]. For example, Kwanghyun Ahn et al. [138] conducted EBSD (Electron Backscatter Diffraction) analyses to quantitatively observe the generation and evolution of deformation twins. Additionally, they investigated the strain rate effect on the strain hardening by both tensile and compressive tests at strain rates ranging from 0.001 s-1 to

10 s-1. The twin modes operating in α-cp titanium (the hcp structure stable below 882ºC) were identified as early as 1953 by the group of J.P. Hammond [139]. Their report reveal that twinning in Ti enables massive crystal shear due to a local reorientation of the crystal lattice. The sense of the applied stress state (i.e., directionality) as the main driving force for twin growth is related to the stress state and this is important in less symmetric crystals, such as Ti. Moreover, the shear stress for the formation or growth of a twin can only enable the crystal to change shape in one direction and therefore the deformation per twin volume is high. This implies that twin growth can only be done through twin lengthening or twin thickening. Although twins grow at the interfaces, theydid not observed basal slip or {101¯2} twinning at temperatures as high as 815°C, however, considerable twinning was observed on {112¯1} and {112¯2} planes in coarse-grained specimens deformed in tension at 815°C. Thus, for the same temperature, if the grains are coarser they will be easier to get twinned than if the grains are small.

b) Fe and Fe-based SMAs

The most common Ti-Ni-based SMAs are very expensive owing to the high-cost of Ti element and the low cold workability of these alloys. Fe and Fe-based SMAs are far less expensive and therefore could be of potential engineering interest if the cost-effectiveness was improved. For example, except for single-crystalline Fe-30Mn-1Si wt.% steel showing 9 % RS (recovery strain) [82], and melt-spun Fe-16Mn-5Cr-6Ni-3Si-0.2B wt.% steel thin foil showing 7.2% RS [147], Fe based SMAs fabricated through conventional processes such as Fe-Mn-Si, [148], Fe-Ni-C [149] and Fe-Ni-Co-Ti [150] suffer from a low recovery strain (< 3%). This can explain the great interest in studying the influence of strain rate and temperature as critical factors in controlling twinning stress in Fe based SMAs.

Recently, the importance of large recovery strain in Fe-Mn-Si-based shape memory steels obtained by annealing was discussed by Y.H. Wen et al. [151]. The results indicate that the shape memory capacity of Fe–Mn–Si based SMAs varies with the annealing temperature. High annealing temperature favours the transformation from austenitic phase to epsilon martensite because of reduced density of dislocation structures, while low temperatures retard this transformation [152]. The volume fraction of the stress induced martensite is affected by both M_s and Neel temperature (T_n) in Fe–Mn–Si. The Neel temperature is the magnetic transformation temperature from a paramagnetic to antiferromagnetic phase with increasing Mn content. Below T_n antiferromagnetic order takes place thus stabilizing austenite and suppressing martensitic transformation [153].

However the percentage of recoverable strain in Fe–Mn–Si SMAs is small and this has prompted to alloy Fe–Mn–Si based SMAs to improve their shape memory behaviour [154].

Combining high strain and thermal treatment can result in an increased shape memory effect on Fe–Mn–Si–Cr–Ni alloys by producing thin plates of reversible epsilon martensite [155]. Applying high strain rate during pre-deformation of Fe–Mn–Si based SMA containing Nb carbide (NbC) above room temperature, also increases shape recovery and recovery stress. This favours the generation of nucleation sites for NbC particles to precipitate, which further promotes martensite formation and reversion [156]. However, the deformation at room temperature did not reach the same percentage of shape recovery as the one tested above room temperature due to the large increase in recovery stress during cooling [157].

c) Cu- and Cu-based SMAs

Cu based alloys have wide transformation temperature range, large superelastic effect, small hysteresis and high damping coefficient. However, the critical transformation stress is highly dependent on the composition. A small change in composition results in large changes in transformation temperatures. The advantage of being able to change the transformation temperature by changing the composition is that the material can be tailored to attain the desired phase at the application temperature. All of these desirable properties have widened the potential applications of Cu-based SMAs, including improving the ductility of Bulk Metallic Glasses (BMGs) with addition of a crystalline shape memory B2 phase.

The critical stress for twinning Cu SMAs is also related to the dependence on strain rate and temperature. In regards to the strain rate, numerous studies have been carried out on the dynamic uniaxial compressive mechanical behaviour of Cu SMAs by means of stress relaxation tests. However, most experimental results indicate that these alloys exhibit apparent strain-rate-softening (i.e. negative SRS) when the strain rate is beyond a critical range. This behaviour has been proven to decrease and stabilize for a large number of cycles [158]. Increased strain rate causes an increase in stresses upon loading and unloading with a narrow resultant hysteretic loop, thus resulting in an overall decrease in the energy dissipation capacity. This is mainly due to self-heating of specimens upon cycling since this requires a larger stress to induce a martensitic state. According to Duerig and co-workers [21], the negative strain rates effect is strongly dependent on the previous thermomechanical history. They observed that when testing Ni-Ti and in Cu-Zn-Al_2 alloys

at increasing strain rates and conditions, they become more adiabatic. This effect can become quite substantial, often causing a temperature rise upon deformation of well over 5°C. A similar temperature drop upon unloading was also observed. Duerig and co-workers [21] also observed that although the transformation temperatures of most Cu-based SMAs such as Cu-Zn-Al and Cu-Al-Ni can be manipulated over a wide temperature range, the practical upper limits are usually 120°C and 200°C, respectively, since above these temperatures the transformations tend to be unstable due to rapid aging effects.

3. Twinning in metallic glass composites.

Deformation twinning is an important mode of plastic deformation that has been observed to strongly influence the microstructural development and mechanical behavior in many crystalline solids. In particular from analysis of literature data, it is largely believed that the stress required for martensitic transformation to occur is controlled mainly by the intimate connection between twinning nucleation and growth. This has led to the incorporation of deformation twinning into polycrystal plasticity models [159]. Highlights include the pioneering model that Chin et al. [160] proposed for face centered cubic materials, where each twinning system is associated with a critical resolved shear stress and where twin growth is governed by Schmid's law [161]. A number of workers have pointed out the favourable effect of twinning on the ductility of hcp metals. For example, Yoo [38] noted that it is those hcp metals that display profuse twinning (e.g. Ti, Zr, Re) that possess higher ductility. Twinning has opened up new avenues for enhanced performance in novel alloys for engineering applications. Several 'super-functional' materials referred to as advance materials, which combine unique engineering properties, are now being processed for commercial use. A class of advance material which has attracted high interest over the last years is shape memory alloys. Shape memory alloys (SMAs) are primarily characterized by the capacity to restore their original dimensional integrity (pre-deformed shape and size) after undergoing substantial deformation when heated up to a certain temperatura [162]. Some crucial use of twinning in novel alloys and other engineering applications will be highlighed in this next section. A relatively new class of materials is called metallic glass, where the liquid is cooled rapidly enough to avoid crystallization. The first reported metallic glass was a 75 at. % Au and 25 at. % Si foil produced in 1960 by Pol Duwez and his colleagues at Caltech [163]. To obtain the material with a fully amorphous structure, high cooling rates, in the order of 10^6 K/s and achievable

by melt-spinning, restrict the morphology of the samples to small foils or ribbons of 20-50 μm thickness [164]. Over the years, new metallic glasses with higher glass forming ability have been developed, and this has enabled to obtain the material in bulk shape (i.e., at least of 1 mm thickness). Metallic glasses exhibit interesting properties such as low Young modulus, high strength, high stored energy, etc. However, the main drackback is that the plastic flow concentrates into a single shear band across the sample upon tension, thus resulting in softening (contrary to the hardening expected for metals) [165] and catastrophic failure at room temperature [166]. To overcome the brittleness of monolithic metallic glasses (MGs), different toughnening strategies have been proposed such as developing in-situ and ex-situ metallic glass matrix composites (MGMCs).

a) Design strategies to improve the ductility and toughness

BMG composites are materials consisting of a metallic glass matrix with crystalline phase/s embedded in it. The purpose of the crystalline phase/s is to arrest the catastrophic propagation of shear bands and promoting their multiplication thereby enhancing toughness. These composites therefore can combine the ductility, fracture toughness and plasticity of conventional metals with the high strength of pure BMG. There are three ways to produce these composites [166].

1. In situ composites: the metallic glass is heated up to cause partial devitrification.
2. In situ composites: precipitation of crystalline phase/s during solidification with the remainder melt forms the amorphous glassy matrix.
3. Ex-situ composites: particles are added to the melt prior to casting.

b) Shape memory bulk metallic glass composites

Alloys corresponding to the Cu-Zr system, including binary Cu-Zr melts, exhibit high glass forming ability and therefore can be obtained amorphous in bulk shape after quenching. If the cooling rate is decreased, a cubic primitive austenitic B2-CuZr phase can crystallize and therefore undergo martensitic transformation when subjected to high enough stress, namely, stress induced martensitic transformation. Considering that martensite is harder than austenite, the phase work hardens upon loading thus resulting in an increase of the ductility of the metallic glass composite. This yielding phenomenon was observed for $Cu_{47.5}Zr_{47.5}Al_5$ and $Cu_{47}Zr_{47}Al_6$ at. % BMGs casted into plates, subsequently machined into a dog-bone geometry and tested in tension [19]. This behaviour was associated to precipitation of B2 CuZr nanocrystals and their subsequent

twinning (martensitic transformation) thus resulting in fracture strain values of 2.02 and 2.04 %, respectively. The similar values is associated to the similar volumen fraction of CuZr phase, 17 and 15 vol. % for $Cu_{47.5}Zr_{47.5}Al_5$ and $Cu_{47}Zr_{47}Al_{6,}$ respectively. Martensitic transformation from cubic B2 to monoclinic B19´ has also been detected in similar alloys such as $(Cu_{0.5}Zr_{0.5})_{100-x}Al_x$ [167] and $(Cu_{0.5}Zr_{0.5})_{100-x}Zn_x$ (x= 0, 1.5, 2.5, 4.5, 7, 10 and 14 at. %) BMG composites upon loading [168].

4. Outlook about challenges and proposed solutions

The current low transformation temperature hindrance (> 100 ºC) of the most commercially successful SMA system, near equiatomic Ni–Ti binary alloy, have triggered several studies on possible SMAs with transformation temperatures above 100ºC (high temperature shape memory alloys) [69] . Over the years, several authors have studied high temperature shape memory alloys [169, 170] due to the importance not only for scientific reasons but also for the market pull. However, the majority of them is restricted in scope to the basic metallurgical properties of reported materials and/or focus on only a few alloy systems. Despite the multiple potential applications of SMAS, there are many challenges that have to be overcomed when designing SMAs, including low controllability and stability, low actuation speed, relatively small usable strain, low accuracy, low energy efficiency and narrow bandwidth. These are related on how SMAs work: SMAs exhibit stress-induced martensitic transformation and in order to revert into austenite they have to be heated up beyond the austenite finish temperature. The functional capability of these alloys clearly depends on much more than simply a high transformation temperature due to the intricate microstructural and thermomechanical issues associated with shape memory and superelastic behaviours. Amidst, the critical stress for twinning less common SMA systems, along with the basic mechanisms for manipulating the transformation temperatures through compositional control, heat treatment and thermomechanical processing remains relatively unknown. The abundance of thermal energy at higher temperatures promotes many rate dependent processes that are otherwise inactive at room temperature and creates a series of tough challenges related to thermal and microstructural stability, deformation and creep resistance, recovery, recrystallisation and environmental resistance. Therefore, it is not surprising that despite the intensive research efforts in recent years, the number of unresolved issues is limiting the commercial application of SMAs. An excellent tool to address these challenges in a cost-effective

manner is to develop more sophisticated models that could provide more accurate predictions.

Currently, the number of kinematically enhanced energy relaxation-based constitutive models for displacive phase transformations, with application to shape memory alloys abound. For instance, Bartel et al. [171] presented a model to make predictions of an axial stress temperature, as well as pseudo-elastic and pseudo-plastic response under uniaxial strain and shear loadings. Other approaches and frameworks were commented by Cheikh et al. [172] who suggested that their model is capable of qualitatively predicting the key characteristics of nonlinear, hysteretic SMA response based on the consideration of evolving energy-minimizing microstructural configurations. However, the developed 2D model focused only on the square-to-rectangular transformations of the cubic-to-tetragonal phase transformation. The methodology for thermo-mechanical model development and implementation can be extended to a generalized free energy function [173] to describe different 2D [174] and 3D [175] phase transformations. In this regard, better predictions are expected to be achieved with the generalization of the modelling approach to the fully-three-dimensional case as well as to other crystallographic systems. Furthermore, although the currently developed models provide a qualitative understanding of coupled thermo-mechanical behaviour and martensitic transformations at the nanoscale in SMAs, recent experimental and theoretical studies have shown that nanostructures reveal different properties than their bulk counterparts because of an increase in surface-to-volume ratio and uncoordination at the surface [176]. This uncoordination phenomenon results in excess surface energy of the nanostructures. However, the excess energy can be explicitly incorporated as surface stress in the continuum phase-field model to introduce size-dependent properties in nanostructures, while surface stress can be considered as the sum of surface residual stress and surface stress due to loading of nanostructure. The mesoscale models (similar to atomistic and molecular dynamics simulations) have limitations in the temporal domain due to computational expense. The development of coarse-grained models is required for attaining practical strain rates in numerical simulations. Another essential future goal is the use of more realistic material parameters to provide a quantitative model validation. It is also worthwhile to make the most of the existing computational tools to develop a synergy among different modelling approaches across length scales, which could enable to address the challenges when designing SMAs. These challenges include low controllability and stability, low actuation speed, relatively small usable strain, low accuracy, low energy

efficiency and narrow bandwidth. These are related on how SMAs work: SMAs exhibit stress-induced martensitic transformation and in order to revert into austenite they have to be heated up beyond the austenite finish temperature (A_f). This can be done by applying intense electrical currents (Joule heating) [177] to heat up rapidly enough and provide the required actuation speed. However, the heat experiences difficulty in transferring across the SMA actuator and thus results in a severe bandwidth problem. Since the heat cannot be transferred instantaneously across the thickness of SMA actuator, the temperature and therefore the response may vary depending on the closeness to the source of heat. Having a fast response not only depends on the heating but also on the cooling rate and this also varies with the thickness and thermal conductivity of the alloy [178]. This problem could be tackled through an optimum control of the size and shape of the SMA actuator combined with careful heating (such as using an electrical heating system) and cooling (such as forced air) [179]. When designing SMA actuators one also has to take into consideration that the thermal conductivity is different for austenite (2.8×10^{-2} J (mm S K)$^{-1}$) and martensite (1.4×10^{-2} J (mm S K)$^{-1}$) [178] and therefore the thermal conductivity would change during the stress-induced martensitic transformation.

The high material cost of SMAs can often be compensated by reduction in design and fabrication complexity but since the shape memory behaviour depends on the composition, an important challenge is to develop SMAs with homogeneous composition. For example, when casting SMAs using rapid solidification to retain microalloying elements in solid solution in austenite, the microstructure and composition may vary across the sample since those areas far from the copper mould will cool down more slowly and therefore they are prone to segregation to grain boundaries. This not only results in variation in microstructure and composition across the sample but also to embrittlement. Controlling the mechanical performance through microalloying to tune the twinning propensity has been proven to be very useful to optimise the ductility and the stress at which austenite transforms into martensite [191, 192]. The performance not only depends on the nature but also on the concentration of microalloying element/s retained in solid solution in B2 (austenite) crystalline grains upon quenching. Processing also contributes to the overall cost of the materials, and certain alloys are very difficult to process and can lead to very high overall cost despite very low cost of the raw materials. We propose that these problems could be overcome by developing multiscale architectured SMAs with variation in composition and grain size (i.e., gradient structures) accross the sample by using high pressure torsion [180]. Higher flexibility in microstructural control and therefore

on the performance can be achieved by combining torsion with extrusion [181]. Using this method could counterbalance the natural microstructural and compositional gradient originated upon solidification thus resulting in chemical and microstructural homogeneity across the thickness of the sensor. This could be also of interest if during working conditions SMA actuators are subjected to stress/temperatures conditions that are different at the different parts of the actuator. We therefore propose that the development of multiscale architecture SMAs with composition and grain size gradients can be of great interest to overcome some of the challenges when designing SMAs. In this regard, the development of new models that can accurately predict the performance of gradient multiscale architectures would be an important step forward to design SMAs.

Finally, despite recent progress in the development of effective theoretical models as well as in optimizing experimental validation processes, the knowledge pertaining the determination of the critical stress for twinning in SMAS is far from complete. Thus, there is definitely a need for the appropriate unification of these models for accuracy, clarity to circumvent the seemly inconsistencies within these numerous approaches in experimental and theoretical analyses of critical stress for twinning in the shape memory materials. We have highlighted the core inferences in some of the models. While efforts are being made to optimise particular these models, it is worthwhile that we advance the existing computational tools to develop a synergy among different modelling approaches across length scales. The current discourse is a concise narrative of our current understanding of state of the art techniques and processes of shape memory metallic alloys and their critical stress for twinning and it also poses some thought provoking issues about future research.

Acknowledgements

P. Nnamchi and S. González are grateful to the EPSRC for the first grant EP/P019889/1. A. Younes and S. González acknowledge research support from Northumbria University.

References

[1] A. Ölander, "An electrochemical investigation of solid cadmium-gold alloys," *Journal of the American Chemical Society*, vol. 54, (1932), pp. 3819-3833.

[2] A. B. Greninger and V. Mooradian, "Strain transformation in metastable beta copper-zinc and beta copper-Ti alloys," *AIME TRANS*, vol. 128, (1938), pp. 337-369.

[3] L. B. Vernon and H. M. Vernon, "Process of manufacturing articles of thermoplastic synthetic resins," (1941).

[4] W. J. Buehler, J. Gilfrich, and R. Wiley, "Effect of low-temperature phase changes on the mechanical properties of alloys near composition TiNi," *Journal of applied physics*, vol. 34, (1963), pp. 1475-1477.
[5] D. Stoeckel, "Shape memory actuators for automotive applications," *Materials & Design*, vol. 11, (1990), pp. 302-307, https://doi.org/10.1016/0261-3069(90)90013-A.
[6] A. Bellini, M. Colli, and E. Dragoni, "Mechatronic design of a shape memory alloy actuator for automotive tumble flaps: a case study," *IEEE Transactions on Industrial Electronics*, vol. 56, (2009), pp. 2644-2656.
[7] D. J. Hartl and D. C. Lagoudas, "Aerospace applications of shape memory alloys," *Proceedings of the Institution of Mechanical Engineers, Part G: Journal of Aerospace Engineering*, vol. 221, (2007), pp. 535-552, 10.1243/09544100jaero211.
[8] H. Fujita and H. Toshiyoshi, "Micro actuators and their applications," *Microelectronics Journal*, vol. 29, (1998), pp. 637-640, https://doi.org/10.1016/S0026-2692(98)00027-5.
[9] Y. Furuya and H. Shimada, "Shape memory actuators for robotic applications," *Materials & Design*, vol. 12, (1991), pp. 21-28.
[10] L. Petrini and F. Migliavacca, "Biomedical Applications of Shape Memory Alloys," *Journal of Metallurgy*, vol. 2011, (2011), pp. 1-15, 10.1155/2011/501483.
[11] V. L. Lieva and H. Carla, "Smart clothing: a new life," *International Journal of Clothing Science and Technology*, vol. 16, (2004), pp. 63-72, doi:10.1108/09556220410520360.
[12] R. Z. Valiev, R. K. Islamgaliev, and I. V. Alexandrov, "Bulk nanostructured materials from severe plastic deformation," *Progress in materials science*, vol. 45, (2000), pp. 103-108.
[13] H. C. Rogers, J. P. Hirth, and R. E. e. Reed-Hill, *Deformation twinning; proceedings*. New York, Gordon and Breach Science Publishers, (1964).
[14] J. W. Christian and S. Mahajan, "Deformation twinning," *Progress in materials science*, vol. 39, (1995), pp. 1-157.
[15] Y. Zhu, X. Liao, and X. Wu, "Deformation twinning in nanocrystalline materials," *Progress in Materials Science*, vol. 57, (2012), pp. 1-62.
[16] J. Wang, Z. Zeng, C. R. Weinberger, Z. Zhang, T. Zhu, and S. X. Mao, "In situ atomic-scale observation of twinning-dominated deformation in nanoscale body-centred cubic tungsten," *Nature materials*, vol. 14, (2015), pp. 594-600.
[17] I. Gutierrez-Urrutia and D. Raabe, "Dislocation and twin substructure evolution during strain hardening of an Fe–22 wt.% Mn–0.6 wt.% C TWIP steel observed by electron channeling contrast imaging," *Acta Materialia*, vol. 59, (2011), pp. 6449-6462.
[18] H. Funakubo and J. Kennedy, "Shape memory alloys," *Gordon and Breach, xii+ 275, 15 x 22 cm, Illustrated*, (1987).
[19] S. Pauly, S. Gorantla, G. Wang, U. Kühn, and J. Eckert, "Transformation-mediated ductility in CuZr-based bulk metallic glasses," *Nature materials*, vol. 9, (2010), pp. 473-477.
[20] F. E. Wang, "On the TiNi (Nitinol) Martensitic Transition. Part 1," Naval Ordnance Lab White Oal MD(1972).
[21] T. W. Duerig, K. N. Melton, D. Stockel, and C. M. Wayman, *Engineering aspects of shape memory alloys*, 1st ed. London: Butterworth-Heinemann, (1990).
[22] K. Otsuka and C. M. Wayman, *Shape memory materials*, 1 ed. Cambridge, United Kingdom: Cambridge university press, (1998).
[23] L. Wang, G. Huang, Q. Quan, P. Bassani, E. Mostaed, M. Vedani, *et al.*, "The effect of twinning and detwinning on the mechanical property of AZ31 extruded magnesium alloy during strain-path changes," *Materials & Design*, vol. 63, (2014), pp. 177-184, https://doi.org/10.1016/j.matdes.2014.05.056.
[24] C. Rogers and H. Robertshaw, "Development of a novel smart material," in *Proceedings of the 1988 Winter Annual Meeting of the American Society of Mechanical Engineers*, (1988), pp. 1-5.
[25] M. F. Ashby, "A first report on deformation-mechanism maps," *Acta Metallurgica*, vol. 20, (1972), pp. 887-897, https://doi.org/10.1016/0001-6160(72)90082-X.

[26] C. Bouvet, S. Calloch, and C. Lexcellent, "A phenomenological model for pseudoelasticity of shape memory alloys under multiaxial proportional and nonproportional loadings," *European Journal of Mechanics - A/Solids*, vol. 23, (2004), pp. 37-61, https://doi.org/10.1016/j.euromechsol.2003.09.005.
[27] H. Yan, B. Yang, Y. Zhang, Z. Li, C. Esling, X. Zhao, *et al.*, "Variant organization and mechanical detwinning of modulated martensite in Ni–Mn–In metamagnetic shape-memory alloys," *Acta Materialia*, vol. 111, (2016), pp. 75-84, https://doi.org/10.1016/j.actamat.2016.03.049.
[28] P. K. Kumar and D. C. Lagoudas, "Introduction to Shape Memory Alloys," in *Shape Memory Alloys: Modeling and Engineering Applications*, ed Boston, MA: Springer US, (2008), pp. 1-51, 10.1007/978-0-387-47685-8_1.
[29] E. Orowan, J. S. Kohler, F. Seitz, W. T. Read, and W. Shockley, "Dislocations in metals," *American Institute of Mining and Metallurgical Engineers, New York*, (1954), pp. 116-120.
[30] Y. Zhang, Z. Li, C. Esling, J. Muller, X. Zhao, and L. Zuo, "A general method to determine twinning elements," *Journal of applied crystallography*, vol. 43, (2010), pp. 1426-1430.
[31] R. L. Bell and R. W. Cahn, "The dynamics of twinning and the interrelation of slip and twinning in zinc crystals," *Proc. R. Soc. Lond. A*, vol. 239, (1957), pp. 494-521.
[32] P. Price, "Nucleation and growth of twins in dislocation-free zinc crystals," *Proc. R. Soc. Lond. A*, vol. 260, (1961), pp. 251-262.
[33] J. Christian, "Physics of Strength and Plasticity," *Ed. AS Argon, MIT Press, Cambridge (Mass.) and London*, (1969), pp. 85-91.
[34] B. A. Bilby and J. W. Christian, "The Mechanism of Phase Transformations in Solids," *The Institute of Metals, London*, (1956), pp. 121-172.
[35] J. A. Venables, "The electron microscopy of deformation twinning," *Journal of Physics and Chemistry of Solids*, vol. 25, (1964), pp. 685-692, https://doi.org/10.1016/0022-3697(64)90177-5.
[36] M. Niewczas and G. Saada, "A physics of condensed matter structure defects and mechanical properties," *Philos. Mag. A*, vol. 82, (2002), pp. 167-191.
[37] A. Sleeswyk, "Perfect dislocation pole models for twinning in the fcc and bcc lattices," *Philosophical Magazine*, vol. 29, (1974), pp. 407-421.
[38] M. H. Yoo, "Slip, twinning, and fracture in hexagonal close-packed metals," *Metallurgical Transactions A*, vol. 12, (1981), pp. 409-418, 10.1007/bf02648537.
[39] R. Bell and R. Cahn, "The nucleation problem in deformation twinning," *Acta Metallurgica*, vol. 1, (1953), pp. 752-753.
[40] A. Paxton, P. Gumbsch, and M. Methfessel, "A quantum mechanical calculation of the theoretical strength of metals," *Philosophical Magazine Letters*, vol. 63, (1991), pp. 267-274.
[41] P. Price, "Nonbasal Glide in Dislocation-Free Cadmium Crystals. I. The (101¯1)[12¯10] System," *Journal of Applied Physics*, vol. 32, (1961), pp. 1746-1750.
[42] P. Price, "Pyramidal glide and the formation and climb of dislocation loops in nearly perfect zinc crystals," *Philosophical Magazine*, vol. 5, (1960), pp. 873-886.
[43] A. Cottrell and B. Bilby, "LX. A mechanism for the growth of deformation twins in crystals," *The London, Edinburgh, and Dublin Philosophical Magazine and Journal of Science*, vol. 42, (1951), pp. 573-581.
[44] R. Priestner and W. Leslie, "Nucleation of deformation twins at slip plane intersections in BCC metals," *Philosophical Magazine*, vol. 11, (1965), pp. 895-916.
[45] N. Thompson and D. Millard, "Twin formation, in cadmium," *The London, Edinburgh, and Dublin Philosophical Magazine and Journal of Science*, vol. 43, (1952), pp. 422-440.
[46] F. Frank and W. Read Jr, "Multiplication processes for slow moving dislocations," *Physical Review*, vol. 79, (1950), pp. 722-728.
[47] S. Miura, J.-I. Takamura, and N. Narita, "Orientation dependence of flow stress for twinning in silver crystals," in *Transactions of the Japan Institute of Metals*, (1968), pp. 555-562.
[48] S. Mahajan and G. Chin, "Formation of deformation twins in fcc crystals," *Acta metallurgica*, vol. 21, (1973), pp. 1353-1363.

[49] Y. Zhu, X. Liao, S. Srinivasan, Y. Zhao, M. Baskes, F. Zhou, *et al.*, "Nucleation and growth of deformation twins in nanocrystalline aluminum," *Applied physics letters*, vol. 85, (2004), pp. 5049-5051.
[50] M. Chen, E. Ma, K. J. Hemker, H. Sheng, Y. Wang, and X. Cheng, "Deformation twinning in nanocrystalline aluminum," *Science*, vol. 300, (2003), pp. 1275-1277.
[51] Y. Zhu, J. Narayan, J. Hirth, S. Mahajan, X. Wu, and X. Liao, "Formation of single and multiple deformation twins in nanocrystalline fcc metals," *Acta materialia*, vol. 57, (2009), pp. 3763-3770.
[52] J. P. Hirth and J. Lothe, *Theory of dislocations*, 2nd ed. Malabar, FL: Krieger Pub. Co., (1992).
[53] S. Mahajan, "Nucleation and growth of deformation twins in Mo-35 at.% Re alloy," *Philosophical Magazine*, vol. 26, (1972), pp. 161-171.
[54] A. Sleeswyk, "½< 111> screw dislocations and the nucleation of {112}< 111> twins in the bcc lattice," *Philosophical Magazine*, vol. 8, (1963), pp. 1467-1486.
[55] K. Lagerlöf, "On deformation twinning in bcc metals," *Acta metallurgica et materialia*, vol. 41, (1993), pp. 2143-2151.
[56] S. Mahajan, "Interrelationship between slip and twinning in BCC crystals," *Acta Metallurgica*, vol. 23, (1975), pp. 671-684.
[57] G. Kaschner, C. Tomé, R. McCabe, A. Misra, S. Vogel, and D. Brown, "Exploring the dislocation/twin interactions in zirconium," *Materials Science and Engineering: A*, vol. 463, (2007), pp. 122-127.
[58] L. Wang, P. Eisenlohr, Y. Yang, T. Bieler, and M. Crimp, "Nucleation of paired twins at grain boundaries in titanium," *Scripta Materialia*, vol. 63, (2010), pp. 827-830.
[59] A. Serra, D. Bacon, and R. Pond, "Twins as barriers to basal slip in hexagonal-close-packed metals," *Metallurgical and materials transactions A*, vol. 33, (2002), pp. 809-812.
[60] M. Klassen-Neklyudova, *Twinning during plastic deformation and fracture of crystals*, 1st ed.: Springer, (1964).
[61] K. Otsuka and K. Shimizu, "Pseudoelasticity and shape memory effects in alloys," *International Metals Reviews*, vol. 31, (1986), pp. 93-114.
[62] C. Wayman and K. Shimizu, "The shape memory ('Marmem') effect in alloys," *Metal Science Journal*, vol. 6, (1972), pp. 175-183.
[63] H. E. Karaca, S. M. Saghaian, B. Basaran, G. S. Bigelow, R. D. Noebe, and Y. I. Chumlyakov, "Compressive response of nickel-rich NiTiHf high-temperature shape memory single crystals along the [111] orientation," *Scripta Materialia*, vol. 65, (2011), pp. 577-580, https://doi.org/10.1016/j.scriptamat.2011.06.027.
[64] J. Wang and H. Sehitoglu, "Modelling of martensite slip and twinning in NiTiHf shape memory alloys," *Philosophical Magazine*, vol. 94, (2014), pp. 2297-2317.
[65] K. M. Knowles and D. A. Smith, "The crystallography of the martensitic transformation in equiatomic nickel-titanium," *Acta Metallurgica*, vol. 29, (1981), pp. 101-110, https://doi.org/10.1016/0001-6160(81)90091-2.
[66] Y. Liu and Z. L. Xie, "Twinning and detwinning of 〈0 1 1〉 type II twin in shape memory alloy," *Acta Materialia*, vol. 51, (2003), pp. 5529-5543, https://doi.org/10.1016/S1359-6454(03)00417-8.
[67] J. X. Zhang, M. Sato, and A. Ishida, "Deformation mechanism of martensite in Ti-rich Ti–Ni shape memory alloy thin films," *Acta Materialia*, vol. 54, (2006), pp. 1185-1198, https://doi.org/10.1016/j.actamat.2005.10.046.
[68] C. Zhang, R. H. Zee, and P. E. Thoma, "Development of Ni-Ti based shape memory alloys for actuation and control," in *IECEC 96. Proceedings of the 31st Intersociety Energy Conversion Engineering Conference*, (1996), pp. 239-244 vol.1, 10.1109/IECEC.1996.552877.
[69] J. Ma, I. Karaman, and R. D. Noebe, "High temperature shape memory alloys," *International Materials Reviews*, vol. 55, (2010), pp. 257-315, 10.1179/095066010X12646898728363.
[70] K. Otsuka and X. Ren, "Physical metallurgy of Ti–Ni-based shape memory alloys," *Progress in Materials Science*, vol. 50, (2005), pp. 511-678, https://doi.org/10.1016/j.pmatsci.2004.10.001.

[71] G. S. Firstov, J. Van Humbeeck, and Y. N. Koval, "High Temperature Shape Memory Alloys Problems and Prospects," *Journal of Intelligent Material Systems and Structures*, vol. 17, (2006), pp. 1041-1047, 10.1177/1045389x06063922.
[72] G. S. Bigelow, A. Garg, S. A. Padula, D. J. Gaydosh, and R. D. Noebe, "Load-biased shape-memory and superelastic properties of a precipitation strengthened high-temperature Ni50.3Ti29.7Hf20 alloy," *Scripta Materialia*, vol. 64, (2011), pp. 725-728, https://doi.org/10.1016/j.scriptamat.2010.12.028.
[73] K. C. Atli, I. Karaman, R. D. Noebe, A. Garg, Y. I. Chumlyakov, and I. V. Kireeva, "Improvement in the Shape Memory Response of Ti50.5Ni24.5Pd25 High-Temperature Shape Memory Alloy with Scandium Microalloying," *Metallurgical and Materials Transactions A*, vol. 41, (2010), pp. 2485-2497, 10.1007/s11661-010-0245-z.
[74] B. Kockar, K. C. Atli, J. Ma, M. Haouaoui, I. Karaman, M. Nagasako, *et al.*, "Role of severe plastic deformation on the cyclic reversibility of a Ti50.3Ni33.7Pd16 high temperature shape memory alloy," *Acta Materialia*, vol. 58, (2010), pp. 6411-6420, https://doi.org/10.1016/j.actamat.2010.08.003.
[75] V. Vítek, "Intrinsic stacking faults in body-centred cubic crystals," *The Philosophical Magazine: A Journal of Theoretical Experimental and Applied Physics*, vol. 18, (1968), pp. 773-786, 10.1080/14786436808227500.
[76] X. L. Meng, W. Cai, L. M. Wang, Y. F. Zheng, L. C. Zhao, and L. M. Zhou, "Microstructure of stress-induced martensite in a Ti–Ni–Hf high temperature shape memory alloy," *Scripta Materialia*, vol. 45, (2001), pp. 1177-1182, https://doi.org/10.1016/S1359-6462(01)01147-2.
[77] Y. Teng, S. Zhu, F. Wang, and W. Wu, "Electronic structures and shape-memory behavior of Ti50Ni50−xCux (x=0, 6.25, 12.5, 18.75 and 25.0at%) by density functional theory," *Physica B: Condensed Matter*, vol. 393, (2007), pp. 18-23, https://doi.org/10.1016/j.physb.2006.12.012.
[78] L. Gou, Y. Liu, and T. Ng, "Effect of Cu Content on Atomic Positions of Ti50Ni50−xCux Shape Memory Alloys Based on Density Functional Theory Calculations," *Metals*, vol. 5, (2015), p. 2222.
[79] I. M. Khan, H. Y. Kim, T.-h. Nam, and S. Miyazaki, "Effect of Cu addition on the high temperature shape memory properties of Ti50Ni25Pd25 alloy," *Journal of Alloys and Compounds*, vol. 577, (2013), pp. S383-S387, https://doi.org/10.1016/j.jallcom.2011.12.116.
[80] C. M. Wayman, "On memory effects related to martensitic transformations and observations in β-brass and Fe3Pt," *Scripta Metallurgica*, vol. 5, (1971), pp. 489-492, https://doi.org/10.1016/0036-9748(71)90097-4.
[81] J. Wang and N. Stanford, "A critical assessment of work hardening in TWIP steels through micropillar compression," *Materials Science and Engineering: A*, vol. 696, (2017), pp. 42-51.
[82] A. Sato, E. Chishima, K. Soma, and T. Mori, "Shape memory effect in γ⇄ ϵ transformation in Fe-30Mn-1Si alloy single crystals," *Acta Metallurgica*, vol. 30, (1982), pp. 1177-1183.
[83] Y. Tanaka, Y. Himuro, R. Kainuma, Y. Sutou, T. Omori, and K. Ishida, "Ferrous polycrystalline shape-memory alloy showing huge superelasticity," *Science*, vol. 327, (2010), pp. 1488-1490.
[84] T. Omori, K. Ando, M. Okano, X. Xu, Y. Tanaka, I. Ohnuma, *et al.*, "Superelastic effect in polycrystalline ferrous alloys," *Science*, vol. 333, (2011), pp. 68-71.
[85] A. Ojha and H. Sehitoglu, "Twinning stress prediction in bcc metals and alloys," *Philosophical Magazine Letters*, vol. 94, (2014), pp. 647-657.
[86] A. Ojha, H. Sehitoglu, L. Patriarca, and H. Maier, "Twin nucleation in Fe-based bcc alloys—modeling and experiments," *Modelling and Simulation in Materials Science and Engineering*, vol. 22, (2014), pp. 075010-1-075010-21.
[87] M. Guerioune, Y. Amiour, W. Bounour, O. Guellati, A. Benaldjia, A. Amara, *et al.*, "SHS of shape memory CuZnAl alloys," *International Journal of Self-Propagating High-Temperature Synthesis*, vol. 17, (2008), pp. 41-48.
[88] S. Alkan, Y. Wu, A. Ojha, and H. Sehitoglu, "Transformation stress of shape memory alloy CuZnAl: Non-Schmid behavior," *Acta Materialia*, vol. 149, (2018), pp. 220-234.

[89] R. Liu, Z. J. Zhang, L. L. Li, X. H. An, and Z. F. Zhang, "Microscopic mechanisms contributing to the synchronous improvement of strength and plasticity (SISP) for TWIP copper alloys," *Scientific Reports*, vol. 5, (2015), pp. 1-7, 10.1038/srep09550.
[90] D. Han, Z. Y. Wang, Y. Yan, F. Shi, and X. W. Li, "A good strength-ductility match in Cu-Mn alloys with high stacking fault energies: Determinant effect of short range ordering," *Scripta Materialia*, vol. 133, (2017), pp. 59-64, 10.1016/j.scriptamat.2017.02.010.
[91] S. Asgari, E. El-Danaf, S. R. Kalidindi, and R. D. Doherty, "Strain hardening regimes and microstructural evolution during large strain compression of low stacking fault energy fcc alloys that form deformation twins," *Metallurgical and Materials Transactions. A, Physical Metallurgy and Materials Science*, vol. 28, (1997), pp. 1781-1796, 10.1007/s11661-997-0109-3.
[92] T. Duerig, "The use of superelasticity in modern medicine," *MRS Bulletin (USA)*, vol. 27, (2002), pp. 101-104.
[93] M. Sanati, R. C. Albers, and F. J. Pinski, "Electronic and crystal structure of NiTi martensite," *Physical Review B*, vol. 58, (1998), pp. 13590-13593, 10.1103/PhysRevB.58.13590.
[94] Y. Y. Ye, C. T. Chan, and K. M. Ho, "Structural and electronic properties of the martensitic alloys TiNi, TiPd, and TiPt," *Physical Review B*, vol. 56, (1997), pp. 3678-3689, 10.1103/PhysRevB.56.3678.
[95] S. Miyazaki, H. Y. Kim, and H. Hosoda, "Development and characterization of Ni-free Ti-base shape memory and superelastic alloys," *Materials Science & Engineering A*, vol. 438, (2006), pp. 18-24, 10.1016/j.msea.2006.02.054.
[96] H. Y. Kim, Y. Ikehara, J. I. Kim, H. Hosoda, and S. Miyazaki, "Martensitic transformation, shape memory effect and superelasticity of Ti–Nb binary alloys," *Acta Materialia*, vol. 54, (2006), pp. 2419-2429, 10.1016/j.actamat.2006.01.019.
[97] K. A. Bywater and J. W. Christian, "Martensitic transformations in titanium-tantalum alloys," *The Philosophical Magazine: A Journal of Theoretical Experimental and Applied Physics*, vol. 25, (1972), pp. 1249-1273, 10.1080/14786437208223852.
[98] A. Ojha and H. Sehitoglu, "Critical Stresses for Twinning, Slip, and Transformation in Ti-Based Shape Memory Alloys," *Shape Memory and Superelasticity*, vol. 2, (2016), pp. 180-195, 10.1007/s40830-016-0061-4.
[99] H. Kim, J. Fu, H. Tobe, J. Kim, and S. Miyazaki, "Crystal Structure, Transformation Strain, and Superelastic Property of Ti–Nb–Zr and Ti–Nb–Ta Alloys," *Shape Memory and Superelasticity*, vol. 1, (2015), pp. 107-116, 10.1007/s40830-015-0022-3.
[100] Y. Ogawa, D. Ando, Y. Sutou, and J. Koike, "Aging Effect of Mg-Sc Alloy with α+β Two-Phase Microstructure," *MATERIALS TRANSACTIONS*, vol. 57, (2016), pp. 1119-1123, 10.2320/matertrans.M2016093.
[101] D. Ando, Y. Ogawa, T. Suzuki, Y. Sutou, and J. Koike, "Age-hardening effect by phase transformation of high Sc containing Mg alloy," *Materials Letters*, vol. 161, (2015), pp. 5-8, 10.1016/j.matlet.2015.06.057.
[102] Y. Ogawa, D. Ando, Y. Sutou, and J. Koike, "A lightweight shape-memory magnesium alloy," *Science*, vol. 353, (2016), pp. 368-370, 10.1126/science.aaf6524.
[103] R. W. Armstrong and P. J. Worthington, "A Constitutive Relation for Deformation Twinning in Body Centered Cubic Metals," in *Metallurgical Effects at High Strain Rates*, R. W. Rohde, B. M. Butcher, J. R. Holland, and C. H. Karnes, Eds., ed Boston, MA: Springer US, (1973), pp. 401-414, 10.1007/978-1-4615-8696-8_22.
[104] W. Z. Han, S. D. Wu, S. X. Li, and Z. F. Zhang, "Origin of deformation twinning from grain boundary in copper," *Applied Physics Letters*, vol. 92, (2008), pp. 221909-1-221909-3, 10.1063/1.2938881.
[105] B. Roy, N. Kumar, P. Nambissan, and J. Das, "Evolution and interaction of twins, dislocations and stacking faults in rolled alpha-brass during nanostructuring at sub-zero temperature," *Aip Advances*, vol. 4, (2014), pp. 067101-1-067101-8, 10.1063/1.4881376.
[106] S. Zherebtsov, G. Dyakonov, G. Salishchev, A. Salem, and S. Semiatin, "The Influence of Grain Size on Twinning and Microstructure Refinement During Cold Rolling of Commercial-Purity Titanium,"

Metallurgical and Materials Transactions, vol. 47, (2016), pp. 5101-5113, 10.1007/s11661-016-3679-0.
[107] X. L. Wu, K. M. Youssef, C. C. Koch, S. N. Mathaudhu, L. J. Kecskés, and Y. T. Zhu, "Deformation twinning in a nanocrystalline hcp Mg alloy," *Scripta Materialia*, vol. 64, (2011), pp. 213-216, 10.1016/j.scriptamat.2010.10.024.
[108] K. M. Rahman, V. A. Vorontsov, and D. Dye, "The effect of grain size on the twin initiation stress in a TWIP steel," *Acta Materialia*, vol. 89, (2015), pp. 247-257, 10.1016/j.actamat.2015.02.008.
[109] M. A. Meyers, O. Vöhringer, and V. A. Lubarda, "The onset of twinning in metals: a constitutive description," *Acta Materialia*, vol. 49, (2001), pp. 4025-4039, 10.1016/S1359-6454(01)00300-7.
[110] M. Nishida, K. Yamauchi, A. Chiba, and Y. Higashi, "International Conference on Martensitic Transformations : ICOMAT 95,," Lausanne, Switzerland, 1995.
[111] C. Chluba, W. Ge, T. Dankwort, C. Bechtold, R. L. de Miranda, L. Kienle, *et al.*, "Effect of crystallographic compatibility and grain size on the functional fatigue of sputtered TiNiCuCo thin films," *Philosophical transactions. Series A, Mathematical, physical, and engineering sciences*, vol. 374, (2016), pp. 20150311-1-20150311-14, 10.1098/rsta.2015.0311.
[112] J. Harding, "The yield and fracture behaviour of high-purity iron single crystals at high rates of strain," *Proceedings of the Royal Society of London. Series A. Mathematical and Physical Sciences*, vol. 299, (1967), pp. 464-490.
[113] I. Gutierrez-Urrutia, S. Zaefferer, and D. Raabe, "The effect of grain size and grain orientation on deformation twinning in a Fe–22 wt.% Mn–0.6 wt.% C TWIP steel," *Materials Science & Engineering A*, vol. 527, (2010), pp. 3552-3560, 10.1016/j.msea.2010.02.041.
[114] N. Naeita and J. Takamura, "Deformation twinning in silver-and copper-alloy crystals," *The Philosophical Magazine: A Journal of Theoretical Experimental and Applied Physics*, vol. 29, (1974), pp. 1001-1028, 10.1080/14786437408226586.
[115] R. Ueji, N. Tsuchida, D. Terada, N. Tsuji, Y. Tanaka, A. Takemura, *et al.*, "Tensile properties and twinning behavior of high manganese austenitic steel with fine-grained structure," *Scripta Materialia*, vol. 59, (2008), pp. 963-966, 10.1016/j.scriptamat.2008.06.050.
[116] S. Vercammen, B. Blanpain, B. C. De Cooman, and P. Wollants, "Cold rolling behaviour of an austenitic Fe–30Mn–3Al–3Si TWIP-steel: the importance of deformation twinning," *Acta Materialia*, vol. 52, (2004), pp. 2005-2012, 10.1016/j.actamat.2003.12.040.
[117] S. Tan, J. Lao, and S. Yang, "Influence of grain size on shape memory effect of polycrystalline Fe□Mn□Si alloys," *Scripta Metallurgica et Materialia*, vol. 25, (1991), pp. 2613-2615, https://doi.org/10.1016/0956-716X(91)90078-F.
[118] K. K. Jee, W. Y. Jang, Y. H. Chung, and M. C. Shin, "Effect of Microstructure on Shape-Memory Effect in Fe-32Mn-6.5Si Alloy," *Materials Science Forum*, vol. 394-395, (2002), pp. 423-426, 10.4028/www.scientific.net/MSF.394-395.423.
[119] J. Wan and S. Chen, "Martensitic transformation and shape memory effect in Fe–Mn–Si based alloys," *Current Opinion in Solid State & Materials Science*, vol. 9, (2005), pp. 303-312, 10.1016/j.cossms.2006.07.005.
[120] M. Murakami, H. Otsuka, and S. Matsuda, "Improvement in shape memory effect for Fe-Mn-Si alloys," in *Transactions of the Iron and Steel Institute of Japan*, (1987), pp. B89-B89.
[121] Q. Gu, J. Van Humbeeck, and L. Delaey, "A review on the martensitic transformation and shape memory effect in Fe-Mn-Si alloys," *Le Journal de Physique IV*, vol. 4, (1994), pp. C3-135-C3-144.
[122] G. Wang, H. Peng, C. Zhang, S. Wang, and Y. Wen, "Relationship among grain size, annealing twins and shape memory effect in fe–mn–si based shape memory alloys," *Smart Materials and Structures*, vol. 25, (2016), pp. 075013-1-075013-9, 10.1088/0964-1726/25/7/075013.
[123] S. Mahajan, C. Pande, M. Imam, and B. Rath, "Formation of annealing twins in fcc crystals," *Acta Materialia (USA)*, vol. 45, (1997), pp. 2633-2638.
[124] C. S. Pande, B. B. Rath, and M. A. Imam, "Effect of annealing twins on Hall–Petch relation in polycrystalline materials," *Materials Science & Engineering A*, vol. 367, (2004), pp. 171-175, 10.1016/j.msea.2003.09.100.

[125] S. Mahajan, "Critique of mechanisms of formation of deformation, annealing and growth twins: Face-centered cubic metals and alloys," *Scripta Materialia*, vol. 68, (2013), pp. 95-99, 10.1016/j.scriptamat.2012.09.011.
[126] T. Blewitt, R. Coltman, and J. Redman, "Low-temperature deformation of copper single crystals," *Journal of Applied Physics*, vol. 28, (1957), pp. 651-660.
[127] R. L. Nolder and G. Thomas, "The substructure of plastically deformed nickel," *Acta Metallurgica*, vol. 12, (1964), pp. 227-240.
[128] E. El-Danaf, S. R. Kalidindi, and R. D. Doherty, "Influence of grain size and stacking-fault energy on deformation twinning in fcc metals," *Metallurgical and Materials Transactions. A, Physical Metallurgy and Materials Science*, vol. 30, (1999), pp. 1223-1234, 10.1007/s11661-999-0272-9.
[129] J. R. Cahoon, Q. Li, and N. L. Richards, "Microstructural and processing factors influencing the formation of annealing twins," *Materials Science & Engineering A*, vol. 526, (2009), pp. 56-61, 10.1016/j.msea.2009.07.021.
[130] C. X. Huang, K. Wang, S. D. Wu, Z. F. Zhang, G. Y. Li, and S. X. Li, "Deformation twinning in polycrystalline copper at room temperature and low strain rate," *Acta Materialia*, vol. 54, (2006), pp. 655-665, 10.1016/j.actamat.2005.10.002.
[131] Y. Zhu, X. Liao, X. Wu, and J. Narayan, "Grain size effect on deformation twinning and detwinning," *Journal of Materials Science*, vol. 48, (2013), pp. 4467-4475, 10.1007/s10853-013-7140-0.
[132] C. S. Pande and K. P. Cooper, "Nanomechanics of Hall–Petch relationship in nanocrystalline materials," *Progress in Materials Science*, vol. 54, (2009), pp. 689-706, 10.1016/j.pmatsci.2009.03.008.
[133] X. Wu and Y. Zhu, "Inverse grain-size effect on twinning in nanocrystalline Ni," *Physical review letters*, vol. 101, (2008), pp. 025503-1-025503-8.
[134] J.-Y. Zhang, G. Liu, R. H. Wang, J. Li, J. Sun, and E. Ma, "Double-inverse grain size dependence of deformation twinning in nanocrystalline Cu," *Physical Review B*, vol. 81, (2010), pp. 172104-1-172104-8.
[135] S. Zherebtsov, G. Dyakonov, A. Salem, V. Sokolenko, G. Salishchev, and S. Semiatin, "Formation of nanostructures in commercial-purity titanium via cryorolling," *Acta Materialia*, vol. 61, (2013), pp. 1167-1178.
[136] Y. Qian, S. Zhi-Wei, L. Ju, H. Xiaoxu, X. Lin, S. Jun, *et al.*, "Strong crystal size effect on deformation twinning," *Nature*, vol. 463, (2010), pp. 335-338, 10.1038/nature08692.
[137] S. Mahajan and D. F. Williams, "Deformation Twinning in Metals and Alloys," *International Metallurgical Reviews*, vol. 18, (1973), pp. 43-61, 10.1179/imtlr.1973.18.2.43.
[138] R. Reed-Hill, "Role of deformation twinning in determining the mechanical properties of metals," in *The Inhomogeneity of Plastic Deformation*, *ASM Seminar*, (1973), pp. 285-311.
[139] G. F. Bolling and R. H. Richman, "Continual mechanical twinning: Part I: Formal description," *Acta Metallurgica*, vol. 13, (1965), pp. 709-722, https://doi.org/10.1016/0001-6160(65)90136-7.
[140] W. Koester and M. O. Speidel, "The influence of temperature and grain size on the marked yield linit of copper alloys," *Z METALLKD*, vol. 56, (1965), pp. 585-598.
[141] W. W. Chen, Q. Wu, J. H. Kang, and N. A. Winfree, "Compressive superelastic behavior of a NiTi shape memory alloy at strain rates of 0.001–750 s− 1," *International Journal of Solids and Structures*, vol. 38, (2001), pp. 8989-8998.
[142] S. Nemat-Nasser, J. Yong Choi, W.-G. Guo, J. B. Isaacs, and M. Taya, "High Strain-Rate, Small Strain Response of a NiTi Shape-Memory Alloy," *Journal of Engineering Materials and Technology*, vol. 127, (2005), pp. 83-89, 10.1115/1.1839215.
[143] P. Wollants, J. Roos, and L. Delaey, "OF EQUILIBRIUM," *Progress in Materials Science*, vol. 37, (1993), pp. 227-288.
[144] R. Kapoor and S. Nemat-Nasser, "Determination of temperature rise during high strain rate deformation," *Mechanics of Materials*, vol. 27, (1998), pp. 1-12, 10.1016/S0167-6636(97)00036-7.

[145] Y. Liu, J. v. Humbeeck, Y. Li, and K. T. Ramesh, "High strain rate deformation of martensitic NiTi shape memory alloy," *Scripta Materialia*, (1999), pp. Medium: X; Size: pp. 89-95.
[146] Y. Liu, Y. Li, and K. T. Ramesh, "Rate dependence of deformation mechanisms in a shape memory alloy," *Philosophical Magazine A*, vol. 82, (2002), pp. 2461-2473, 10.1080/01418610208240046.
[147] T. Masuya, N. Yoneyama, S. Kumai, and A. Sato, "Grain size effect on the microstructure of deformed Fe-Mn-Si based shape memory alloys," in *Materials science forum*, (2000), pp. 267-270.
[148] Y. Wen, H. Peng, D. Raabe, I. Gutiérrez-Urrutia, J. Chen, and Y. Du, "Large recovery strain in Fe-Mn-Si-based shape memory steels obtained by engineering annealing twin boundaries," *Nature communications*, vol. 5, (2014), p. 4964.
[149] S. Kajiwara and T. Kikuchi, "Shape memory effect and related transformation behavior in Fe□ Ni□ C alloys," *Acta Metallurgica et Materialia*, vol. 38, (1990), pp. 847-855.
[150] Y. Koval, V. Kokorin, and L. Khandros, "The Shape-Memory Effect in Iron--Nickel--Cobalt--Titanium Alloys," *Fiz. Met. Metalloved.*, vol. 48, (1979), pp. 1309-1311.
[151] Y. H. Wen, H. B. Peng, D. Raabe, I. Gutierrez-Urrutia, J. Chen, and Y. Y. Du, "Large recovery strain in Fe-Mn-Si-based shape memory steels obtained by engineering annealing twin boundaries," *Nature Communications*, vol. 5, (2014), pp. 4964-1-4964-9, 10.1038/ncomms5964.
[152] H. Li, D. Dunne, and N. Kennon, "Factors influencing shape memory effect and phase transformation behaviour of Fe–Mn–Si based shape memory alloys," *Materials Science & Engineering A*, vol. 273, (1999), pp. 517-523, 10.1016/S0921-5093(99)00391-3.
[153] L. Huijun, "The development of new iron based shape memory alloys," Department of Materials Engineering, University of Wollongong, 1996.
[154] T. Hsu, "Fe-Mn-Si based shape memory alloys," in *Materials science forum*, (2000), pp. 199-206.
[155] N. Bergeon, S. Kajiwara, and T. Kikuchi, "Atomic force microscope study of stress-induced martensite formation and its reverse transformation in a thermomechanically treated Fe–Mn–Si–Cr–Ni alloy," *Acta Materialia*, vol. 48, (2000), pp. 4053-4064, 10.1016/S1359-6454(00)00187-7.
[156] A. Baruj, T. Kikuchi, S. Kajiwara, and N. Shinya, "Effect of pre-deformation of austenite on shape memory properties in Fe-Mn-Si-based alloys containing Nb and C," *Materials Transactions*, vol. 43, (2002), pp. 585-588.
[157] A. Baruj, T. Kikuchi, S. Kajiwara, and N. Shinya, "Improved shape memory properties and internal structures in Fe-Mn-Si-based alloys containing Nb and C," in *Journal de Physique IV (Proceedings)*, (2003), pp. 373-376.
[158] S. Miyazaki, T. Imai, Y. Igo, and K. Otsuka, "Effect of cyclic deformation on the pseudoelasticity characteristics of Ti-Ni alloys," *Metallurgical transactions A*, vol. 17, (1986), pp. 115-120.
[159] S. R. Kalidindi, "Modeling the strain hardening response of low SFE FCC alloys," *International Journal of Plasticity*, vol. 14, (1998), pp. 1265-1277, https://doi.org/10.1016/S0749-6419(98)00054-0.
[160] G. Chin, W. Hosford, and D. Mendorf, "Accommodation of constrained deformation in fcc metals by slip and twinning," *Proc. R. Soc. Lond. A*, vol. 309, (1969), pp. 433-456.
[161] U. F. Kocks, C. N. Tomé, and H.-R. Wenk, *Texture and anisotropy : preferred orientations in polycrystals and their effect on materials properties*. Cambridge, U.K.; New York: Cambridge University Press, (1998).
[162] J. A. Bezjak, "The shape memory effect in systems of Cu based alloys," *Int. J. Innovative Res. Sci. Eng. Technol.*, vol. 2, (2013), pp. 485-492.
[163] W. Klement Jun, R. H. Willens, and P. O. L. Duwez, "Non-crystalline Structure in Solidified Gold–Silicon Alloys," *Nature*, vol. 187, (1960), pp. 869-870, 10.1038/187869b0.
[164] C. Suryanarayana and A. Inoue, *Bulk Metallic Glasses*: CRC Press, (2010).
[165] A. L. Greer, "Metallic glasses," *Science*, vol. 267, (1995), pp. 1947-1953.
[166] C. A. Schuh, T. C. Hufnagel, and U. Ramamurty, "Mechanical behavior of amorphous alloys," *Acta Materialia*, vol. 55, (2007), pp. 4067-4109, https://doi.org/10.1016/j.actamat.2007.01.052.

[167] S. Pauly, J. Das, J. Bednarcik, N. Mattern, K. B. Kim, D. H. Kim, *et al.*, "Deformation-induced martensitic transformation in Cu–Zr–(Al,Ti) bulk metallic glass composites," *Scripta Materialia*, vol. 60, (2009), pp. 431-434, https://doi.org/10.1016/j.scriptamat.2008.11.015.
[168] D. Wu, K. Song, C. Cao, R. Li, G. Wang, Y. Wu, *et al.*, "Deformation-Induced Martensitic Transformation in Cu-Zr-Zn Bulk Metallic Glass Composites," *Metals*, vol. 5, (2015), pp. 2134-2147.
[169] J. Van Humbeeck, "High Temperature Shape Memory Alloys," *Journal of Engineering Materials and Technology*, vol. 121, (1999), pp. 98-101, 10.1115/1.2816006.
[170] K. Otsuka and X. Ren, "Recent developments in the research of shape memory alloys," *Intermetallics*, vol. 7, (1999), pp. 511-528, https://doi.org/10.1016/S0966-9795(98)00070-3.
[171] T. Bartel, B. Kiefer, K. Buckmann, and A. Menzel, "A kinematically-enhanced relaxation scheme for the modeling of displacive phase transformations," *Journal of Intelligent Material Systems and Structures*, vol. 26, (2015), pp. 701-717, 10.1177/1045389x14557507.
[172] C. Cisse, W. Zaki, and T. Ben Zineb, "A review of constitutive models and modeling techniques for shape memory alloys," *International Journal of Plasticity*, vol. 76, (2016), pp. 244-284, https://doi.org/10.1016/j.ijplas.2015.08.006.
[173] R. P. Dhote, H. Gomez, R. N. V. Melnik, and J. Zu, "3D coupled thermo-mechanical phase-field modeling of shape memory alloy dynamics via isogeometric analysis," *Computers & Structures*, vol. 154, (2015), pp. 48-58, https://doi.org/10.1016/j.compstruc.2015.02.017.
[174] D. M. Hatch, T. Lookman, A. Saxena, and S. R. Shenoy, "Proper ferroelastic transitions in two dimensions: Anisotropic long-range kernels, domain wall orientations, and microstructure," *Physical Review B*, vol. 68, (2003), p. 104105, 10.1103/PhysRevB.68.104105.
[175] J. Sapriel, "Domain-wall orientations in ferroelastics," *Physical Review B*, vol. 12, (1975), pp. 5128-5140, 10.1103/PhysRevB.12.5128.
[176] E. Roduner, "Applications: Facts and Fictions," in *Nanoscopic Materials: Size-Dependent Phenomena*, ed: The Royal Society of Chemistry, (2006), pp. 263-280, 10.1039/9781847557636-00263.
[177] R. Featherstone and Y. H. Teh, "Improving the Speed of Shape Memory Alloy Actuators by Faster Electrical Heating," Berlin, Heidelberg, (2006), pp. 67-76.
[178] M. G. Faulkner, J. J. Amalraj, and A. Bhattacharyya, "Experimental determination of thermal and electrical properties of Ni-Ti shape memory wires," *Smart Materials and Structures*, vol. 9, (2000), pp. 632-639.
[179] Y. Tadesse, N. Thayer, and S. Priya, "Tailoring the Response Time of Shape Memory Alloy Wires through Active Cooling and Pre-stress," *Journal of Intelligent Material Systems and Structures*, vol. 21, (2010), pp. 19-40, 10.1177/1045389x09352814.
[180] J. Y. Kang, J. G. Kim, H. W. Park, and H. S. Kim, "Multiscale architectured materials with composition and grain size gradients manufactured using high-pressure torsion," *Scientific Reports*, vol. 6, (2016), pp. 26590-1-26590-10, 10.1038/srep26590.
[181] O. Bouaziz, H. S. Kim, and Y. Estrin, "Architecturing of Metal-Based Composites with Concurrent Nanostructuring: A New Paradigm of Materials Design," *Advanced Engineering Materials*, vol. 15, (2013), pp. 336-340, doi:10.1002/adem.201200261.
[182] P. Chowdhury, H. Sehitoglu, W. Abuzaid, and H. J. Maier, "Mechanical response of low stacking fault energy Co–Ni alloys – Continuum, mesoscopic and atomic level treatments," *International Journal of Plasticity*, vol. 71, (2015), pp. 32-61, https://doi.org/10.1016/j.ijplas.2015.04.003.
[183] J. Wang and H. Sehitoglu, "Twinning stress in shape memory alloys: theory and experiments," *Acta Materialia*, vol. 61, (2013), pp. 6790-6801.
[184] A. Nespoli, S. Besseghini, S. Pittaccio, E. Villa, and S. Viscuso, "The high potential of shape memory alloys in developing miniature mechanical devices: A review on shape memory alloy mini-actuators," *Sensors and Actuators A: Physical*, vol. 158, (2010), pp. 149-160, https://doi.org/10.1016/j.sna.2009.12.020.

[185] J. M. Jani, M. Leary, A. Subic, and M. A. Gibson, "A review of shape memory alloy research, applications and opportunities," *Materials & Design (1980-2015)*, vol. 56, (2014), pp. 1078-1113.
[186] C. Wen-Shao and A. Yoshikazu, "Use of shape-memory alloys in construction: a critical review," in *Proceedings of the Institution of Civil Engineers - Civil Engineering*, (2016), pp. 87-95, 10.1680/jcien.15.00010.
[187] J. Harding, "The yield and fracture of high-purity iron single crystals under repeated tensile impact loading," *Mem Sci Rev Met*, vol. 65, (1968), pp. 245-254.
[188] J. W. Edington and R. E. Smallman, "On mechanical twinning in single crystals of vanadium," *Acta Metallurgica*, vol. 13, (1965), pp. 765-770, https://doi.org/10.1016/0001-6160(65)90140-9.
[189] P. J. Sherwood, F. Guiu, H. C. Kim, and P. L. Pratt, "PLASTIC ANISOTROPY OF TANTALUM, NIOBIUM, AND MOLYBDENUM," *Canadian Journal of Physics*, vol. 45, (1967), pp. 1075-1089, 10.1139/p67-079.
[190] C. Y. Chiem and W. S. Lee, "The influence of dynamic shear loading on plastic deformation and microstructure of tungsten single crystals," *Materials Science and Engineering: A*, vol. 187, (1994), pp. 43-50, https://doi.org/10.1016/0921-5093(94)90329-8.
[191] J. L. Nilles and W. S. Owen, "Deformation twinning of martensite," *Metallurgical and Materials Transactions B*, vol. 3, (1972), pp. 1877-1883, 10.1007/BF02642573.
[192] G. S. Hirowo, T. Mitsuru, and A. Kōichi, "Deformation Twin in Single Crystals of a 3% Vanadium-Iron Alloy," *Japanese Journal of Applied Physics*, vol. 5, (1966), pp. 879-885.

Figure Captions

Fig. 1. Schematic diagram of twinning nucleation mechanism via successive gliding of twinning partials on three parallel (111) fcc planes [182].

Fig. 2. a) Thompson tetrahedron to visualize slip in FCC metals and b) two dimensional representation [51].

Fig. 3. DFT-computed generalized planar fault energy (GPFE) curve for the successive energy barriers of the Co-33%Ni solid solution [182].

Fig. 4 Crystal structures of NiTi (a) B19′ crystal phase, (b) R-phase (i.e. B33), and (c) B2 form [64].

Fig. 5. Critical martensite twinning stress from deformation experiments. The materials are in the fully martensitic phase of Ni_2MnGa 10M, Ni_2FeGa 14M and $L1_0$, and NiTi B19' [183].

Fig. 6. twinning stress for a number of bcc metals and alloys [85].

Figure 7: Schematic description of grain size on critical stress [131] .

Figure 8: Hall-Petch relationship for dislocation slip and twinning [15].

Fig. 9. Temperature insensitive compilation of twinning stress vs temperature for a number of metals (both mono and polycrystals) [109].

Fig. 10. (a) Transition stress of stress-induced martensite formation and (b) variation of the work-hardening rate for NiTi alloy as a function of strain rate under compression [142].

Fig.11. Future perspective on SMA mini-actuators. Comparison between the current technological limit and the ideal characteristics of SMA mini-actuators [184].

Fig. 12: Existing and potential SMA applications in the biomedical domain [185].

Figure 13. Shape-memory alloy bars can be used to connect the two angles placed at both sides of the crack and the shape-memory effect would help to close the crack [186].

Table 1. Experimental and predicted twinning stress for bcc Fe for various twinning mechanisms [86].

Table 2. Comparison of twinning stress obtained in the present study with the ideal and experimental values. Present model yields values twinning stress very close to the experimental values [85].

Table 3: The Hall-Petch slopes for different metallic crystalline structures [131].

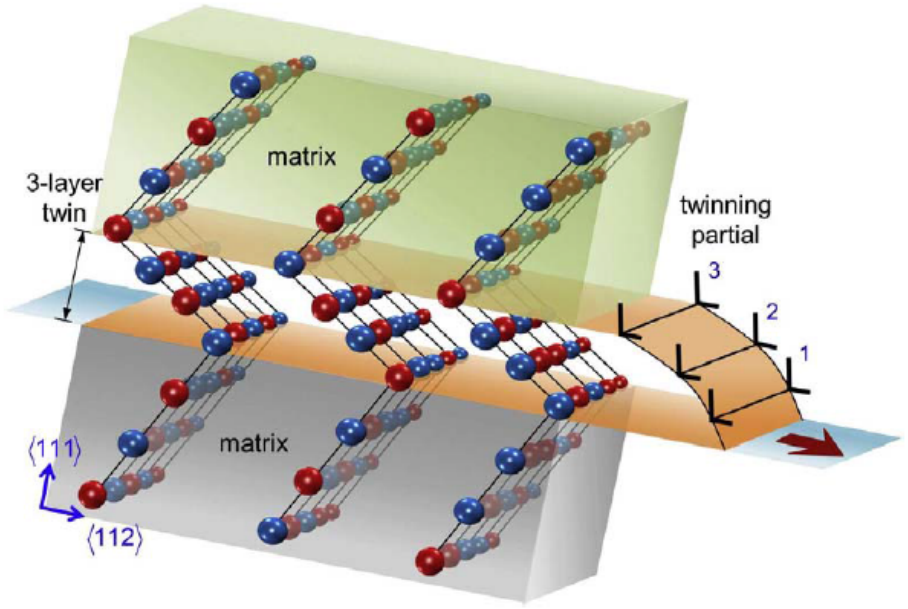

Fig. 1

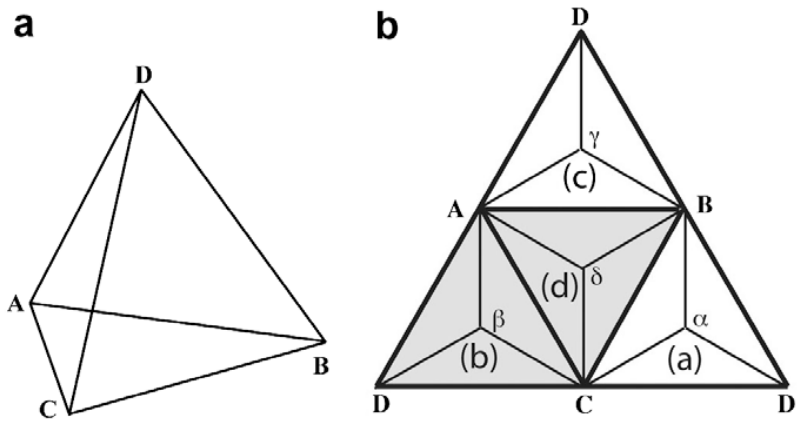

Fig. 2

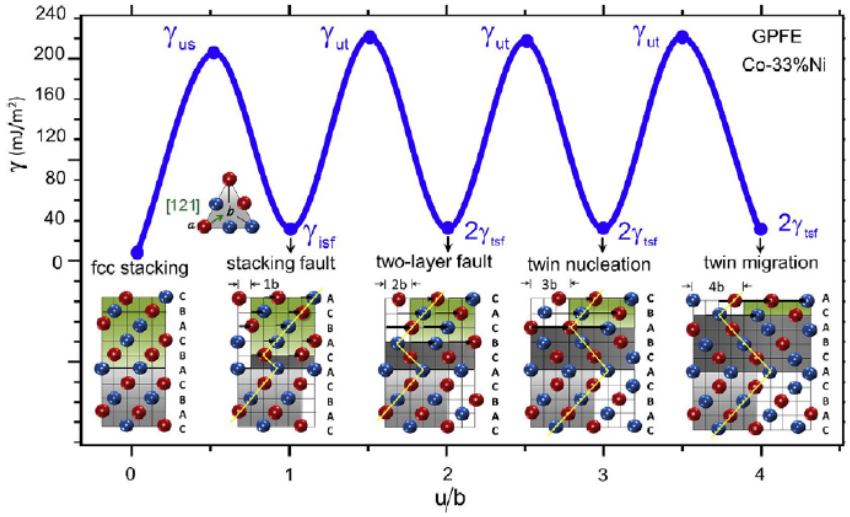
240
200
160
120
80
40
0
γ (mJ/m²)
γus
γut
γut
γut
GPFE
Co-33%Ni
[121]
a
b
γisf
2γtsf
2γtsf
2γtsf
fcc stacking
stacking fault
two-layer fault
twin nucleation
twin migration
1b
2b
3b
4b
0
1
2
3
4
u/b

Fig. 3

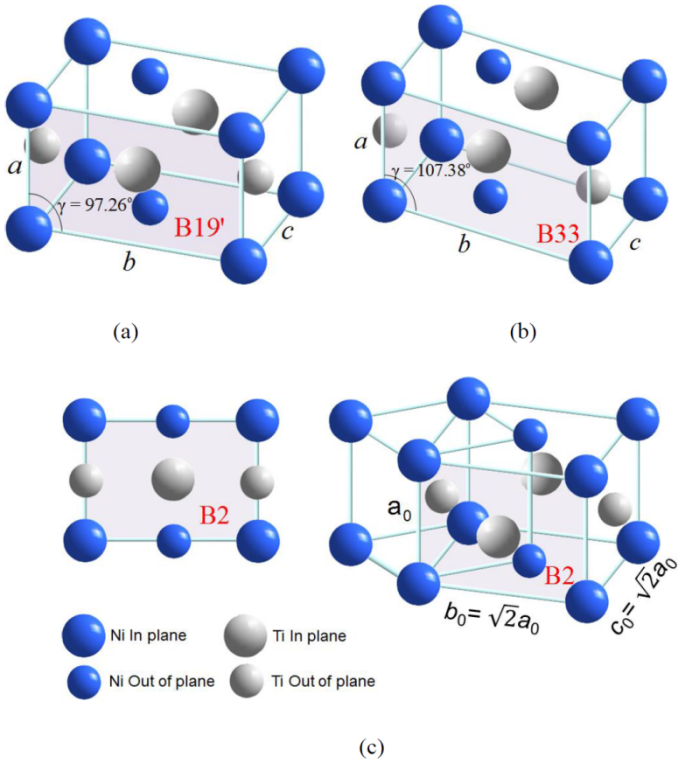
a
γ = 97.26°
B19'
b
c
(a)
a
γ = 107.38°
B33
b
c
(b)
B2
a0
B2
b0= √2a0
c0 = √2a0
Ni In plane
Ti In plane
Ni Out of plane
Ti Out of plane
(c)

Fig. 4

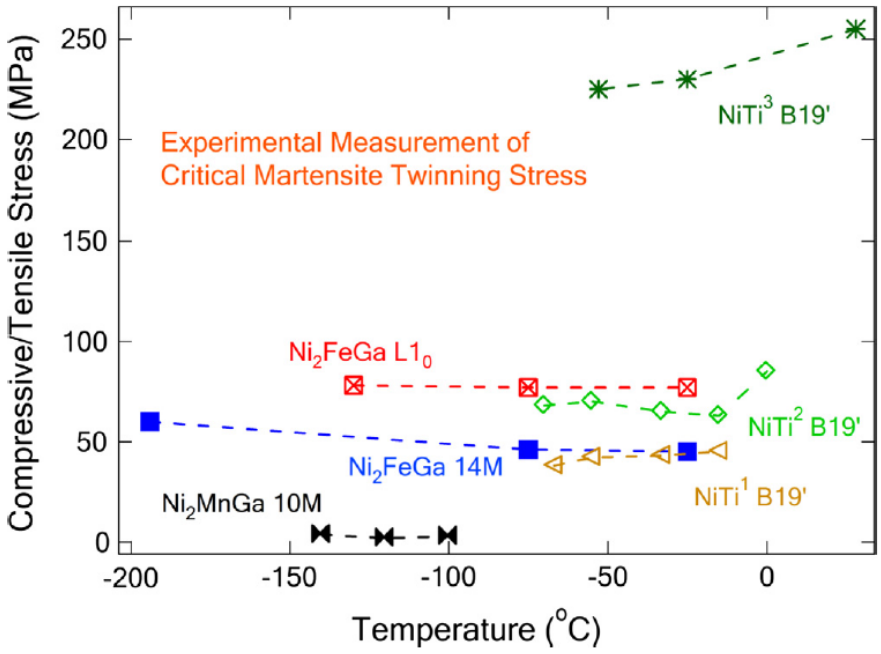
Compressive/Tensile Stress (MPa)
250
200
150
100
50
0
-200
-150
-100
-50
0
Temperature (°C)
Experimental Measurement of
Critical Martensite Twinning Stress
NiTi3 B19'
Ni2FeGa L10
NiTi2 B19'
Ni2FeGa 14M
NiTi1 B19'
Ni2MnGa 10M

Fig. 5

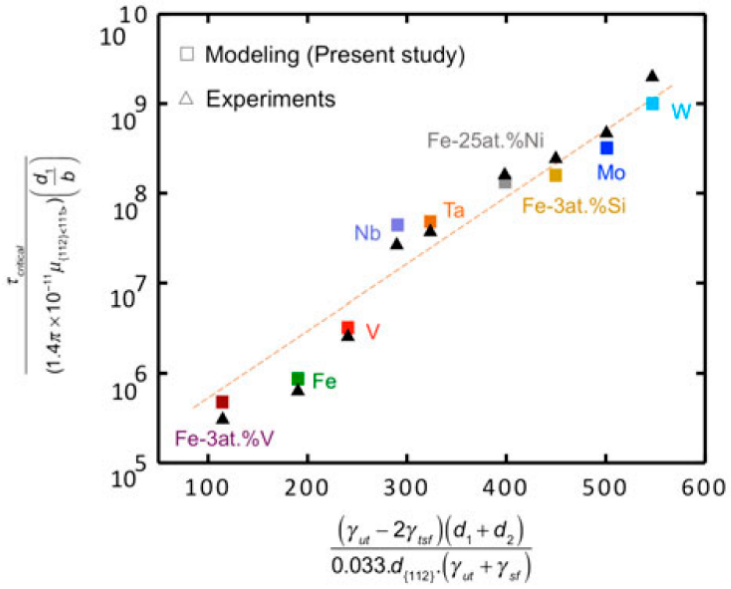
Modeling (Present study)
Experiments
W
Mo
Fe-25at.%Ni
Fe-3at.%Si
Ta
Nb
V
Fe
Fe-3at.%V
$\frac{\tau_{critical}}{(1.4\pi\times10^{-11}\mu_{\{112\}\langle111\rangle})\left(\frac{d_1}{b}\right)}$
$\frac{(\gamma_{ut}-2\gamma_{tsf})(d_1+d_2)}{0.033.d_{\{112\}}.(\gamma_{ut}+\gamma_{sf})}$

Fig. 6

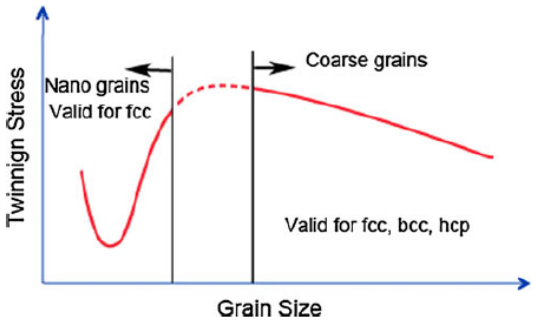
Twinnign Stress
Nano grains
Valid for fcc
Coarse grains
Valid for fcc, bcc, hcp
Grain Size

Fig. 7

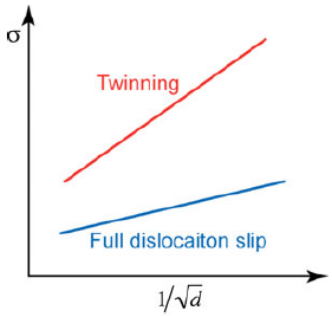

Fig. 8

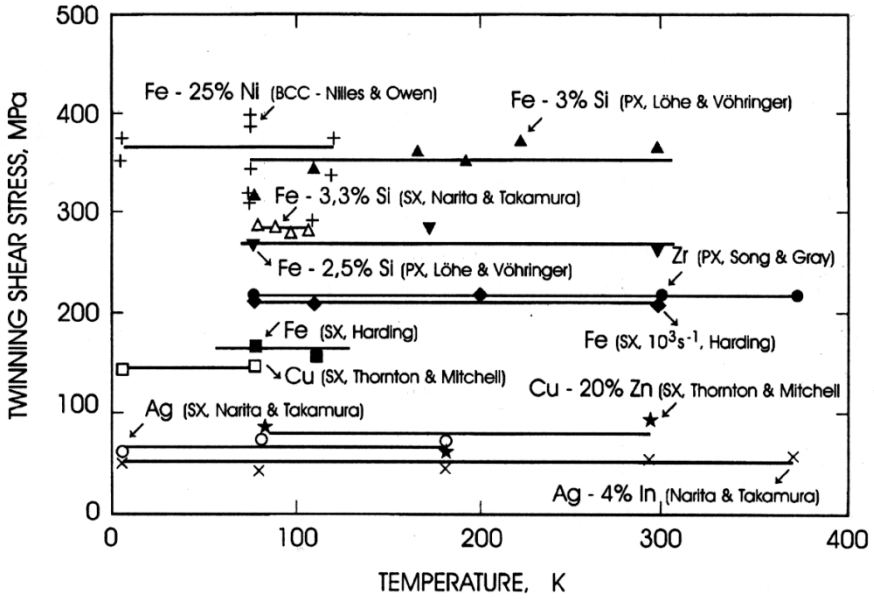
TWINNING SHEAR STRESS, MPa
TEMPERATURE, K
500
400
300
200
100
0
0
100
200
300
400
Fe - 25% Ni (BCC - Nilles & Owen)
Fe - 3% Si (PX, Löhe & Vöhringer)
Fe - 3,3% Si (SX, Narita & Takamura)
Zr (PX, Song & Gray)
Fe - 2,5% Si (PX, Löhe & Vöhringer)
Fe (SX, Harding)
Fe (SX, 10^{3}s^{-1}, Harding)
Cu (SX, Thornton & Mitchell)
Cu - 20% Zn (SX, Thornton & Mitchell)
Ag (SX, Narita & Takamura)
Ag - 4% In (Narita & Takamura)

Fig. 9

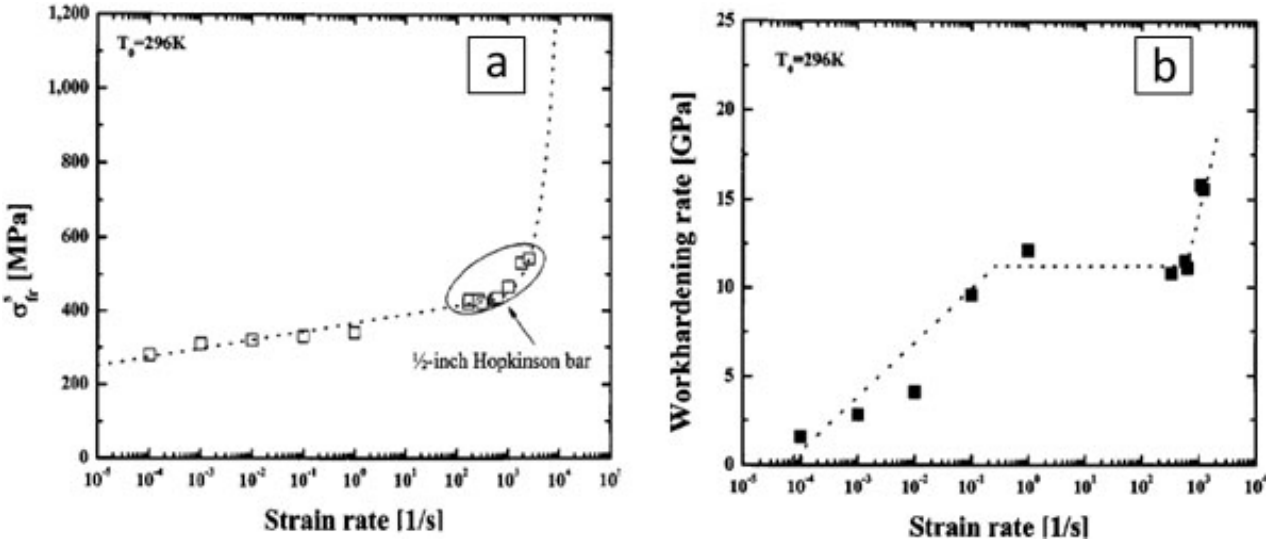
a
T_0=296K
σ^s_{fr} [MPa]
Strain rate [1/s]
½-inch Hopkinson bar
b
T_0=296K
Workhardening rate [GPa]
Strain rate [1/s]

Fig. 10

Table 1

Mechanism/model	Critical twinning stress expression	Predicted (MPa) bcc Fe	Experimental (MPa) bcc Fe
Pole Mechanism	$\tau = \frac{\gamma_{us}}{b}$	7050	170
Dislocation core dissociation	$\tau = \frac{\gamma_{sf}}{3b}$	2500	
Edge dislocation dissociation	$\tau = k_t \frac{\mu}{2\pi(1-\nu)}$	430	
Internal friction stress	$\tau = \tau_o + \frac{1.4\gamma_{sf}}{d}$	7120	
Theoretical	$\tau = \frac{\pi \gamma_{TBM}}{b}$	1530	

Table 2

Metal (bcc)	$\tau_{critical}^{EXp}$ (MPa) (experimental)	$\tau_{critical}^{ideal}$ (MPa) (theory)	$\tau_{critical}^{current}$ (MPa) (present Model)
Fe	170 [112, 187]	1530	190
V	220 [188]	1580	235
Mo	472 [189]	3270	448
Ta	231 [189]	1740	252
Nb	232 [189]	1540	254
W	790 [190]	4530	720
Fe-25at.%Ni	398 [191]	3570	377
Fe-3at.% V	90 [192]	1470	109
Fe-3at.%Si	298 [109]	4040	271

Table 3

Material	k_S for dislocation slip (MPa $m^{1/2}$)	k_T for twinning (MPa $mm^{1/2}$)	k_T/k_s
	fcc		
Cu	5.4 (RT)	21.7 (77 K)	4
Cu–6 wt% Sn	7.1	11.8 (77 K), 7.9 (RT)	1.7, 1.1
Cu–9 wt% Sn	8.2	15.8 (77 K)	1.9
Cu–10 wt% Zn	7.1	11.8 (77 K)	1.7
Cu–15 wt% Zn	8.4	16.7 (295 K)	2.0
	bcc		
Fe–3 wt% Si	12	100	8.3
Armco iron	20	124	6.2
Steel (1010, 1020, 1035)	20	124	6.2
Fe–25 at% Ni	33	100	3.0
Cr	10.1	67.8	6.7
V	3.5	22.4	6.4
	hcp		
Zr	8.3	79.2	9.5
Ti	6	18	3.0

Table 1

Mechanism/model	Critical twinning stress expression	Predicted (MPa) bcc Fe	Experimental (MPa) bcc Fe
Pole Mechanism	$\tau = \frac{\gamma_{us}}{b}$	7050	170
Dislocation core dissociation	$\tau = \frac{\gamma_{sf}}{3b}$	2500	
Edge dislocation dissociation	$\tau = k_t \frac{\mu}{2\pi(1-\nu)}$	430	
Internal friction stress	$\tau = \tau_o + \frac{1.4\gamma_{sf}}{d}$	7120	
Theoretical	$\tau = \frac{\pi \gamma_{TBM}}{b}$	1530	

Table 2

Metal (bcc)	$\tau_{critical}^{EXp}$ (MPa) (experimental)	$\tau_{critical}^{ideal}$ (MPa) (theory)	$\tau_{critical}^{current}$ (MPa) (present Model)
Fe	170 [101, 190]	1530	190
V	220 [191]	1580	235
Mo	472 [192]	3270	448
Ta	231 [192]	1740	252
Nb	232 [192]	1540	254
W	790 [193]	4530	720
Fe-25at.%Ni	398 [194]	3570	377
Fe-3at.% V	90 [195]	1470	109
Fe-3at.%Si	298 [98]	4040	271

Table 3

Material	k_S for dislocation slip (MPa $m^{1/2}$)	k_T for twinning (MPa $mm^{1/2}$)	k_T/k_s
fcc			
Cu	5.4 (RT)	21.7 (77 K)	4
Cu–6 wt% Sn	7.1	11.8 (77 K), 7.9 (RT)	1.7, 1.1
Cu–9 wt% Sn	8.2	15.8 (77 K)	1.9
Cu–10 wt% Zn	7.1	11.8 (77 K)	1.7
Cu–15 wt% Zn	8.4	16.7 (295 K)	2.0
bcc			
Fe–3 wt% Si	12	100	8.3
Armco iron	20	124	6.2
Steel (1010, 1020, 1035)	20	124	6.2
Fe–25 at% Ni	33	100	3.0
Cr	10.1	67.8	6.7
V	3.5	22.4	6.4
hcp			
Zr	8.3	79.2	9.5
Ti	6	18	3.0

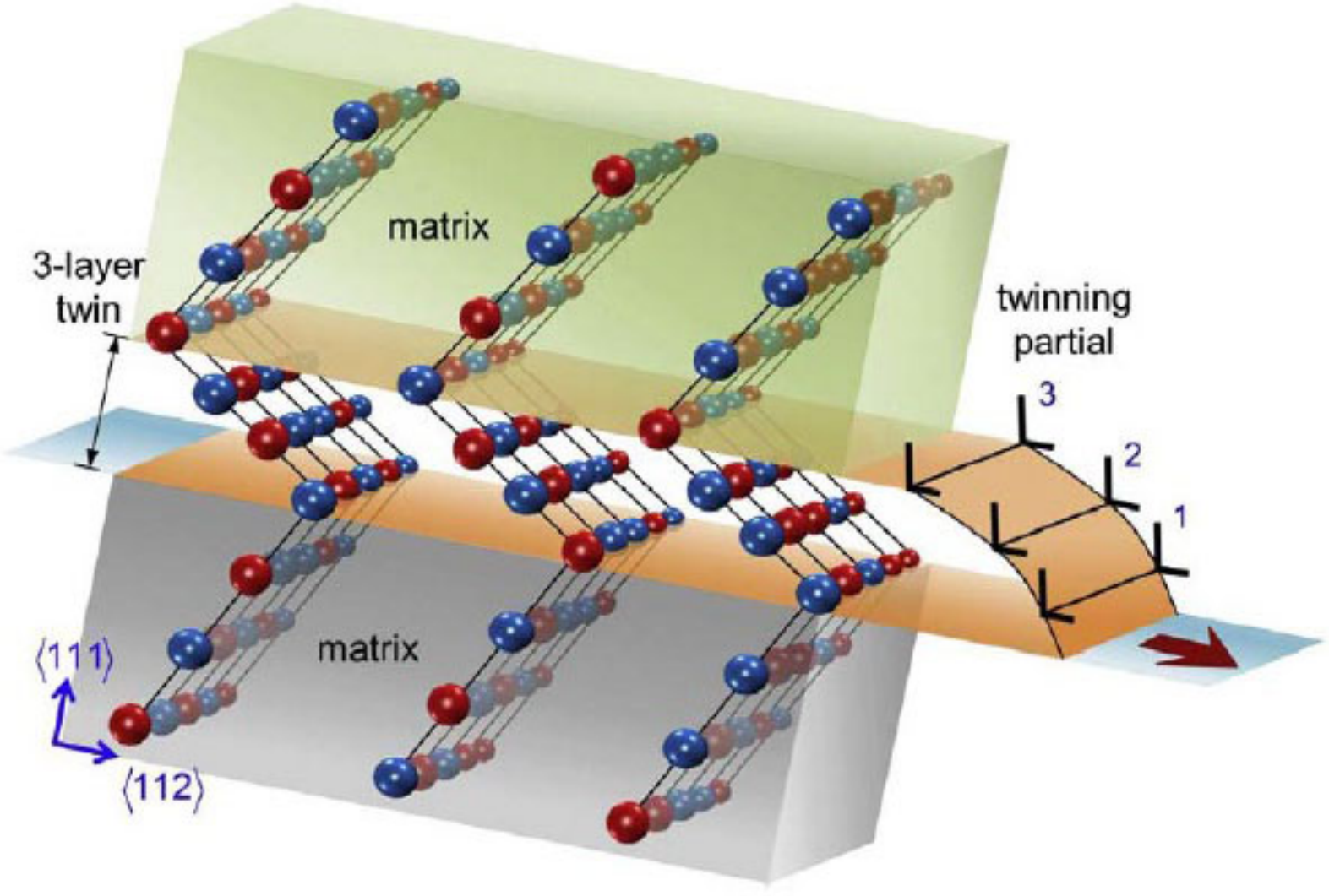
matrix
3-layer
twin
twinning
partial
3
2
1
matrix
⟨111⟩
⟨112⟩

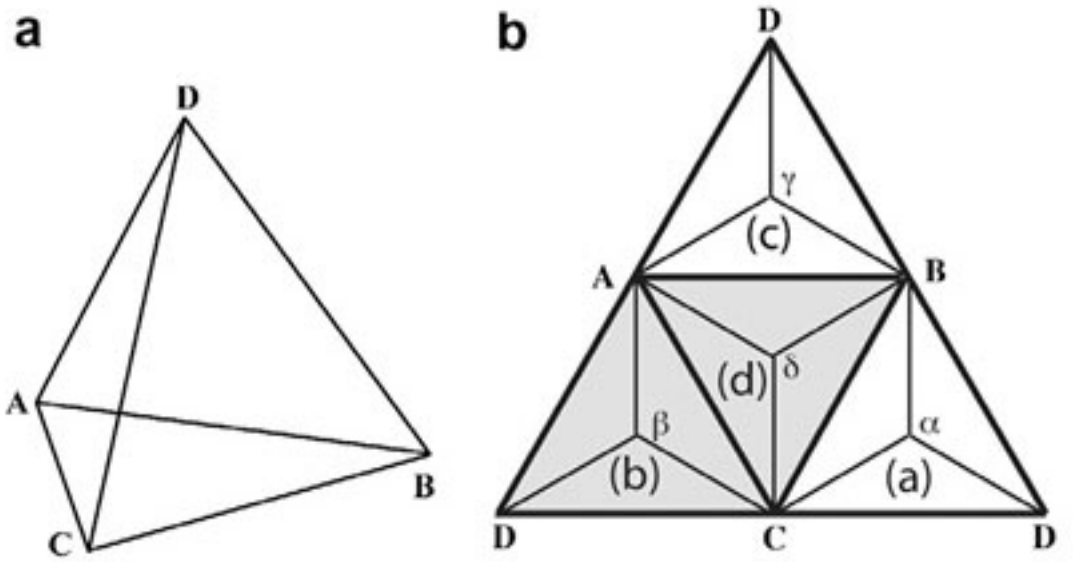
a
D
A
B
C
b
D
γ
(c)
A
B
(d)
δ
β
α
(b)
(a)
D
C
D

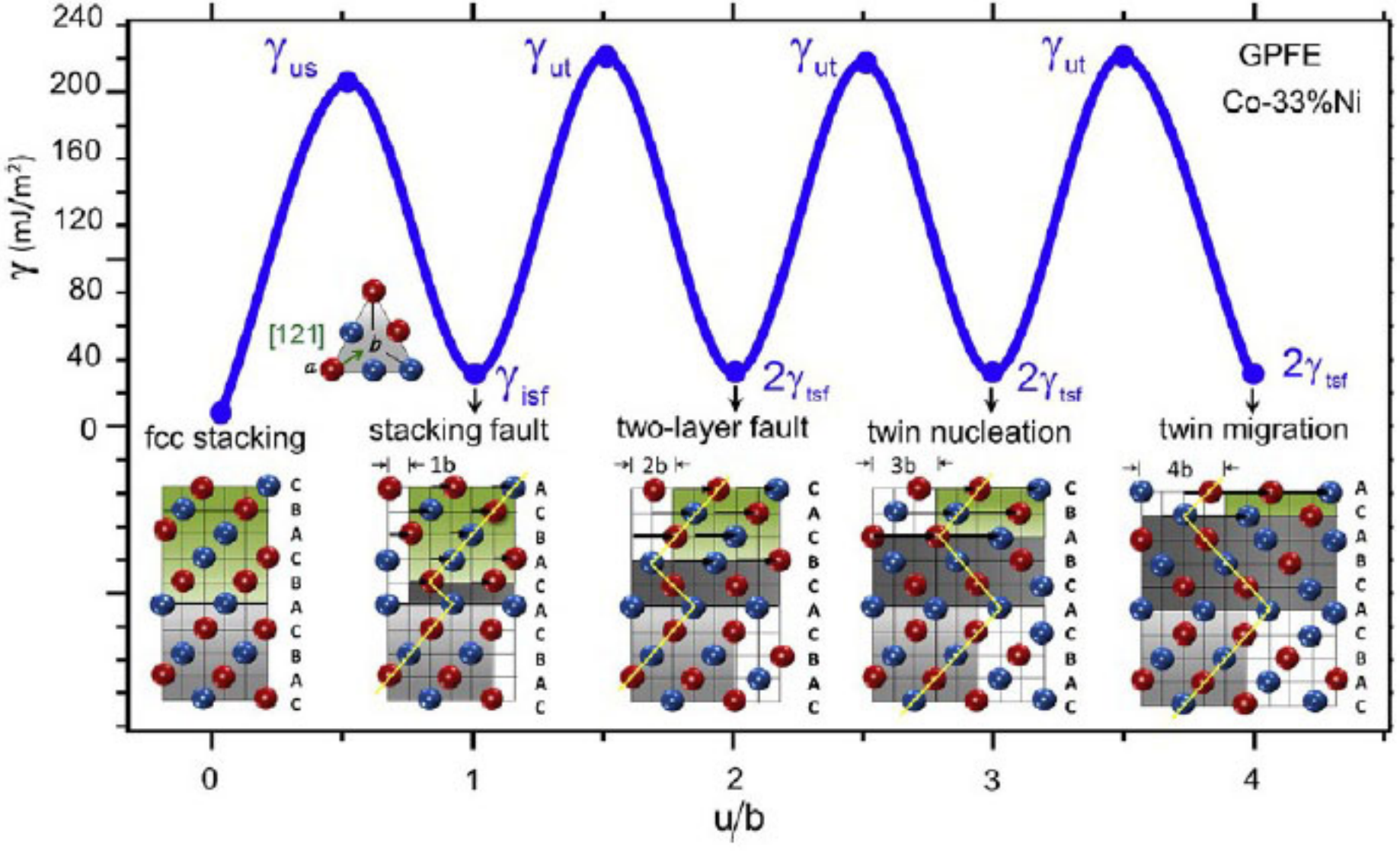
240
200
160
120
80
40
0
γ (mJ/m²)
γus
γut
γut
γut
GPFE
Co-33%Ni
[121]
b
a
γisf
2γtsf
2γtsf
2γtsf
fcc stacking
stacking fault
two-layer fault
twin nucleation
twin migration
1b
2b
3b
4b
0
1
2
3
4
u/b

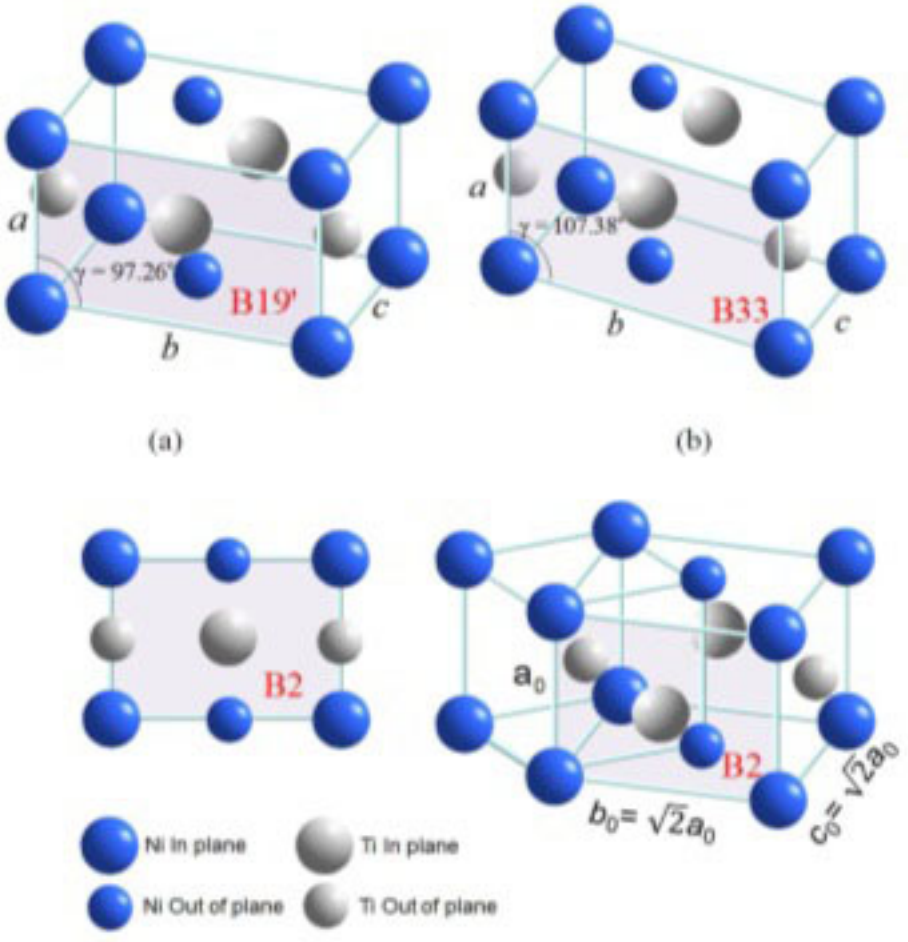
a
γ = 97.26°
B19'
b
c
a
γ = 107.38°
B33
b
c
B2
a0
B2
b0= √2a0
c0= √2a0
Ni In plane
Ti In plane
Ni Out of plane
Ti Out of plane

(a) (b)

(c)

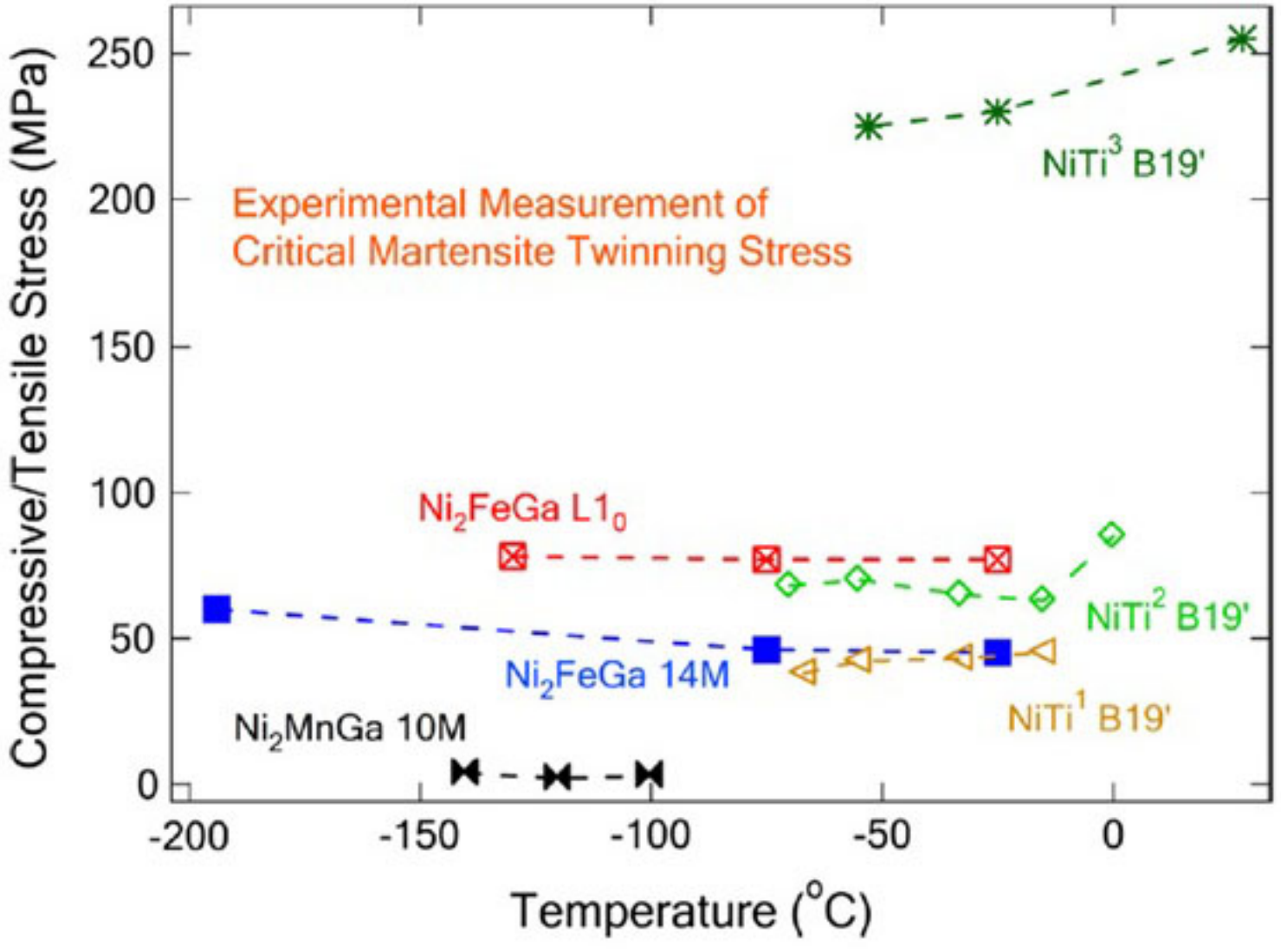
Compressive/Tensile Stress (MPa)
250
200
150
100
50
0
-200
-150
-100
-50
0
Temperature (°C)
Experimental Measurement of
Critical Martensite Twinning Stress
NiTi3 B19'
Ni2FeGa L10
NiTi2 B19'
Ni2FeGa 14M
NiTi1 B19'
Ni2MnGa 10M

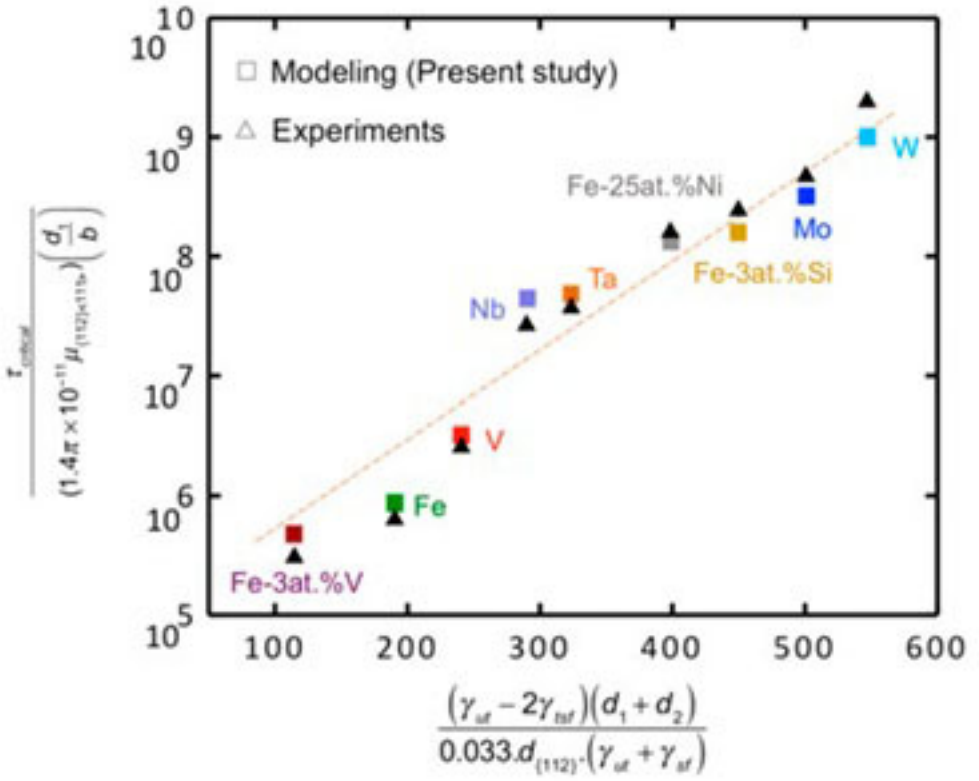
Modeling (Present study)
Experiments
W
Fe-25at.%Ni
Mo
Fe-3at.%Si
Ta
Nb
V
Fe
Fe-3at.%V
$\frac{\tau_{critical}}{(1.4\pi\times10^{-11}\mu_{(112)<111>})\left(\frac{d_1}{b}\right)}$
$\frac{(\gamma_{sf}-2\gamma_{tsf})(d_1+d_2)}{0.033.d_{(112)}.(\gamma_{sf}+\gamma_{sf})}$

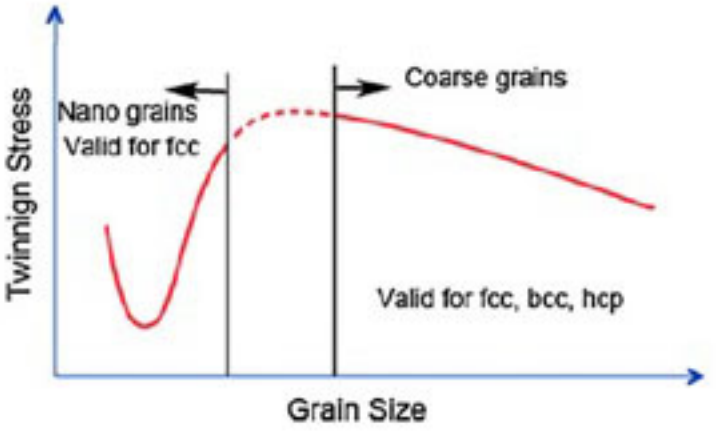
Twinnign Stress
Nano grains
Valid for fcc
Coarse grains
Valid for fcc, bcc, hcp
Grain Size

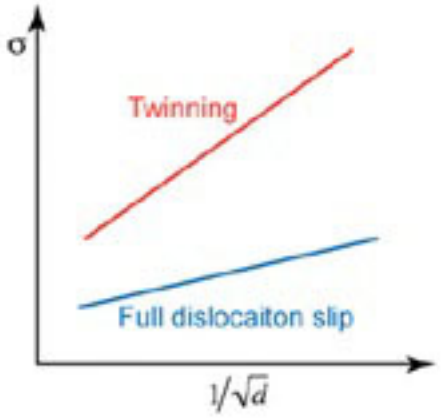
σ
Twinning
Full dislocaiton slip
$1/\sqrt{d}$

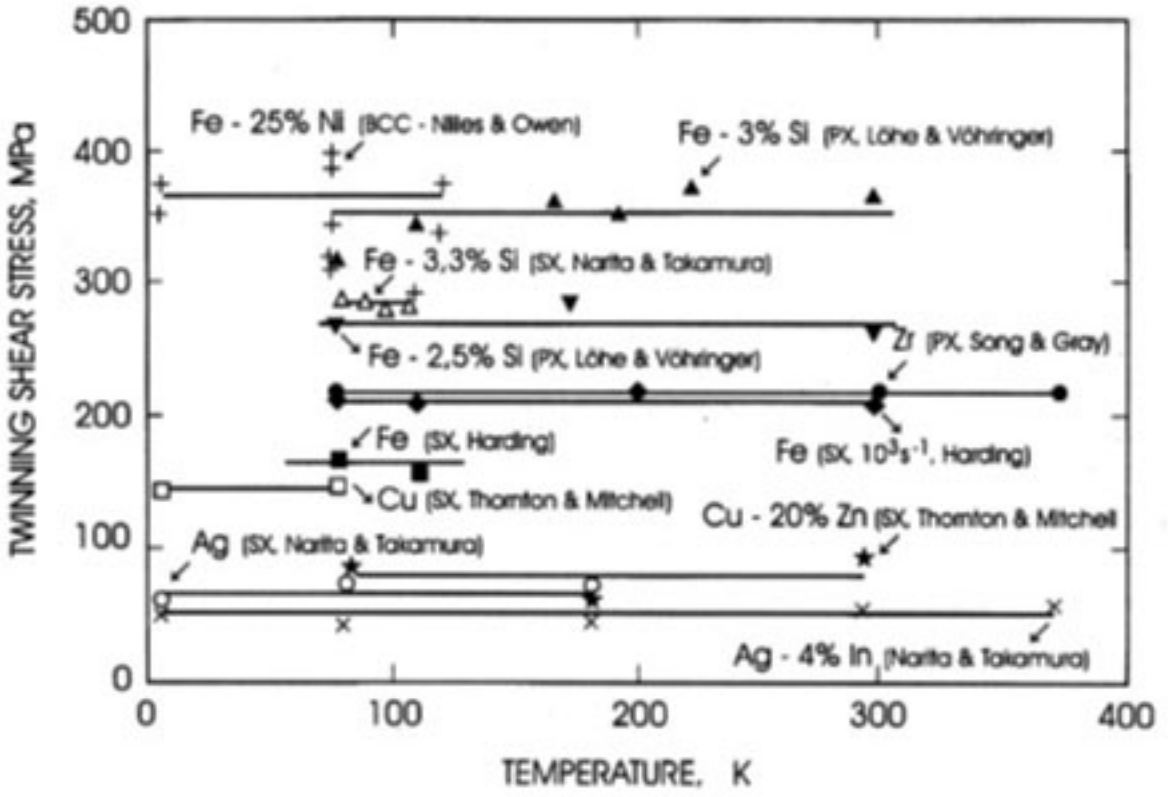
TWINNING SHEAR STRESS, MPa
TEMPERATURE, K
0
100
200
300
400
500
Fe - 25% Ni (BCC - Nilles & Owen)
Fe - 3% Si (PX, Löhe & Vöhringer)
Fe - 3,3% Si (SX, Narita & Takamura)
Fe - 2,5% Si (PX, Löhe & Vöhringer)
Zr (PX, Song & Gray)
Fe (SX, Harding)
Fe (SX, 10^{3}s^{-1}, Harding)
Cu (SX, Thornton & Mitchell)
Cu - 20% Zn (SX, Thornton & Mitchell)
Ag (SX, Narita & Takamura)
Ag - 4% In (Narita & Takamura)